Synthesis of Copper and Calcium Based Metal Organic Frameworks for Biodiesel Production from Waste Cooking Oil

By

Unza Jamil

172147

Session 2016-18

Supervised by

Asst. Prof. Dr. Rabia Liaquat

A Thesis Submitted to the U.S-Pakistan Center for Advanced Studies in Energy in partial fulfillment of the requirements for the degree of

MASTERS of SCIENCE in

ENERGY SYSTEMS ENGINEERING

U.S-Pakistan Center for Advanced Studies in Energy (USPCAS-E)

National University of Sciences and Technology (NUST)

H-12, Islamabad 44000, Pakistan.

August 2019

Synthesis of Copper and Calcium Based Metal Organic Frameworks for Biodiesel Production from Waste Cooking Oil

By

Unza Jamil

172147

Session 2016-18

Supervised by

Asst. Prof. Dr. Rabia Liaquat

A Thesis Submitted to the U.S-Pakistan Center for Advanced Studies in Energy in partial fulfillment of the requirements for the degree of

MASTERS of SCIENCE in

ENERGY SYSTEMS ENGINEERING

U.S-Pakistan Center for Advanced Studies in Energy (USPCAS-E)

National University of Sciences and Technology (NUST)

H-12, Islamabad 44000, Pakistan

August 2019

Thesis Acceptance Certificate

Certified that final copy of MS/MPhil thesis written by **Ms. Unza Jamil**, (Registration No. **172147**), of U.S-Pakistan Center for Advanced Studies in Energy has been vetted by undersigned, found complete in all respects as per NUST Statues/Regulations, is within the similarity indices limit and is accepted as partial fulfillment for the award of MS/MPhil degree. It is further certified that necessary amendments as pointed out by GEC members of the scholar have also been incorporated in the said thesis.

Signature: _____

Name of Supervisor: Dr. Rabia Liaquat

Date: _____

Signature (HoD): _____

Date: _____

Signature (Dean/Principal): _____

Date: _____

Certificate

This is to certify that work in this thesis has been carried out by **Ms. Unza Jamil** and completed under my supervision in Biofuel Energy Laboratory, U.S-Pakistan Center for Advanced Studies in Energy (USPCAS-E), National University of Sciences and Technology, H-12, Islamabad, Pakistan.

Supervisor: _____

Dr. Rabia Liaquat
USPCAS-E
NUST, Islamabad

GEC member # 1: _____

Dr. Naseem Iqbal
USPCAS-E
NUST, Islamabad

GEC member # 2: _____

Dr. Asif Hussain Khoja
USPCAS-E
NUST, Islamabad

GEC member # 3: _____

Dr. M. Bilal Sajid
USPCAS-E
NUST, Islamabad

HoD- (Dept.) _____

Dr. Naseem Iqbal

Principal/ Dean _____

Dr. Zuhair S. Khan
USPCAS-E
NUST, Islamabad

In the eternal memory of my loving parents

Abstract

The increasing use of fossil fuel resources encompasses a burden on the production of overall energy along with continual environmental concerns. The use of biofuels can play a substantial role to contribute for energy production hence waste cooking oil (WCO) utilized for biodiesel production. This study reports the synthesis of copper and calcium based metal organic frameworks (MOFs) as catalysts in the steps of esterification and transesterification. The synthesized catalysts were characterized with XRD, SEM and TGA. XRD results showed sharp characteristics peaks while the crystal size to be 49.04 nm for Cu-MOF while 20.77 nm for Ca-MOF. SEM images showed cubical images of 1.5µm and 2µm for both Cu-MOF and Ca-MOF respectively. TGA results showed that both the materials decomposed at 600°C. The catalysts were then used for their application in the process of biodiesel production from WCO. Furthermore, several standard testing analysis techniques were used to compare the produced samples with standard characteristics of biodiesel such as flashpoint, calorific value and product yield. Flashpoint of Cu-MOF-BD was 130 °C, Ca-MOF-BD was 140 °C and Cu+Ca-MOF-BD was 130.5 °C while calorific value of 40 kJg^{-1} for each with a conversion of 78.33 %, 78 % and 85 % respectively. These synthesized catalysts acted as effective catalyst for biodiesel production process where as the conversion efficiency can be increased further by focusing on optimization of the transesterification and esterification reactions in future studies.

Keywords: Metal organic framework, esterification, transesterification, biodiesel, waste cooking oil.

Table of Contents

List of Figures

List of Tables

List of Journals/Conference Papers

- U. Jamil, R.Mansoor, B. Batool and R. Liaquat "*Photo catalytic Degradation of Organic Dyes by Semiconducting Metal Sulphide Nanoparticles of Copper and Zinc Synthesized through Single Source Precursor*" International workshop on energy materials and nanotechnology (EMNT) 2018 (COMSATS University Islamabad, Abbottabad campus)

List of Abbreviations

BD	Biodiesel
WCO	Waste Cooking Oil
FFA	Free Fatty Acid
FAME	Fatty Acid Methyl Esters
ECC	Economic Coordination Committee
PSO	Pakistan State Oil
AEDB	Alternative Energy Development Board
GCMS	Gas Chromatography Mass Spectrometry
BET	Brunauer Emmett Teller
BDC	Benzene dicarboxylic
MOF	Metal Organic Frameworks
Ca	Calcium
Cu	Copper
DI	Di-Ionized water
DMF	Dimethylforamide
MeOH	Methanol
SEM	Scanning Electron Microscopy
TGA	Thermal Gravimetric Analysis
EDS	Energy Dispersive Spectroscopy
FTIR	Fourier Transform Infrared Spectroscopy
XRD	X-ray Diffraction

Chapter 1

Introduction

1.1 Background

The utilization of fossil fuel resources (coal, oil, natural gas and petrochemical) in comparison to any other is majorly because of its higher energy potential but the increase in non-renewable resource is leading towards the economic stress in terms of fuel prices as a consequence of demand and supply strain [1][2]. Despite of these issues the use of petrochemical fuels is necessary for some very important sectors like transportation, power generation and agriculture. All this scenario will lead to the depletion of these petro reserves and probable environmental problems sue to these fossil fuel reserves hence there is a hype to find out substitute for them [3].The current society system largely relies on the energy obtained from renewable energy resources like fossil fuels as their energy content provision is far higher than any other resource. The major energy requirements around the world are fulfilled by coal, oil, natural gas and petrochemical supplies hence the utilization of fossil fuel resources is increasing day by day on a yearly data basis. This conventional mean of energy production though on one hand is creating a strain between the high price and demand supply gap [2].

As discussed above depletion of petro resources required for transportation along with global warming is one of the major concerns to shift towards the renewable energy resources hence we need an alternative which feasibly fits the requirements [4]. Renewable energy derived from biofuels could be a significant part of this sector and play a vital role to improve the economy and environmental scenarios of the country [5]. Currently a potential amount of alcohol is produced from the sugarcane liquid waste with a potential future upfront from sugarcane crop production [6][7]. Ideally the governmental policies should designate a 10% of share in diesel consumption for blended biodiesel for 2025 though as per current ethanol seems to be a capable option as compared to biodiesel

hence reforms has to be made so that ethanol blended gasoline could be used as vehicle fuel [8]. Certain policies are being proposed to promote the use and production of biofuels which also increase the costs of imported oils. While two main types of biofuels are being produced in practice as ethanol from corn and sugarcane and biodiesel from edible and nonedible oils [9][7].

Due to the high density of diesel fuels in comparison to any other they are generally used for the transportation, power production and agricultural concerns. Biodiesel is one of the comparatively benign options of diesel with its main components as triglycerides which are esters consisting of long chain acids and glycerol forming fatty acids. In specific terms the mono alkyl esters of long chain fatty acids which are being derived from the renewable sources namely vegetable oil or animal fat form biodiesel. This can be utilized for the compression ignition engines [2].

Biodiesel is liquid form of fuel obtained from renewable resources like oil and fats from plant and animal sources through a chemical conversion in the presence of alcohol which alone or in blend with diesel can be used in engines [10]. Biodiesel is a potential alternative for conventional fuels such as diesel due to the comparable properties of flow and combustion with low emission profile [11]. Moreover biodiesel is oxygenated, renewable, biodegradable and environmentally benign fuel. Because of the suitable properties and the environment improvement due to it, many countries pay much attention to Research and Development (R&D) of biodiesel industry and constitute favorable legislation for it. The process of biodiesel production is basically the production of fatty acid methyl esters produced from the conversion of triglycerides in the form of oils and fats combined with an alcohol. Transesterification reaction takes place to complete the conversion process after which the biodiesel sample is collected for further processing which involves washing and drying of the biodiesel sample to prepare it for utilization.

Biodiesel production is a potential alternative with three generations of substrate materials to perform the process of transesterification [12]. The first generation is of edible plants e.g, corns and soyabeans, second generation involving cellulose in nonedible plants e.g, wood, organic waste, food crop waste, specific biomass crops. Third generation is of substrates which are grown for improvements in production biomass e.g algae. In specific

reference to biodiesel production there are a number of variant plant species which can be used for biodiesel production as their seeds are rich in oil e.g., *Pongamia pinnata*, *Cannabus, Jutropha* and *Ricinus commnis* [13].

Vegetable oil after repetitive use for food preparation is referred as waste cooking oil (WCO) which cannot be used for further consumption because the free fatty acid (FFA) content has increased. Disposing this oil leads to several health and environmental pollution problems hence the renewable energy research targets this oil usage for biodiesel production being a cheap feedstock [14]. The qualities of waste cooking oil vary depending on what conditions they are being used to prepare food like temperature and time for frying. Any water content in the waste cooking oil can lead to hydrolysis or saponification due to high FFA content during the process of transesterification [15].

The mechanism of transesterification involves a reaction between a lipid and an alcohol to form esters with glycerol as a byproduct. This is a reversible reaction where its stability towards product side is ensured by the use of excess alcohol. The standard stoichiometry of transesterification is 3:1 for alcohol to lipids but it is sometimes increased e.g., 6:1 to increase the amount of product yield. Transesterification involves three consecutive reversible steps starting with conversion of triglycerides into diglycerides then to monoglycerides. Finally the monoglycerides are converted into glycerol. Here one ester molecule is yielded from each glyceride at each step. The equilibrium of the reaction lies towards production of the fatty acid esters and glycerol though the reactions are reversible [16].

Biodiesel is prepared with an alcohol in the presence of a catalyst by trans-esterifying vegetable oils and animal fats [17][2]. During the process of biodiesel production there are several contributing factors which effect the yield of the product such as reaction time and temperature, oil to alcohol ratio, percentage of catalyst used and stirring speed. In case of waste cooking a two-step conversion process is required namely esterification followed by transesterification where the former one is basically a pretreatment step to purify the substrate oil consisting of unknown composition and a higher number of free fatty acid content. The reaction of esterification requires acidic

catalyst while a basic catalyst is a best fit for transesterification reaction while improvement and optimization is always needed while using different catalysts [18].

The catalyst involved in the process of transesterification has a substantial effect on the reaction considerably increasing the speed of the reaction. In comparison to acidic catalysts which perform the reaction on high temperature like 100 °C and hours of reaction time, the basic catalysts are in contrary and complete the reaction at room temperature even. The commonly used alkalis are the hydroxides of sodium and potassium, carbonates and alkoxides like methoxide, ethoxide, propoxide and butoxide [19].

Methanol, ethanol and butanol are the short chain alcohols which are usually employed in the transesterification reaction. The cost and efficiency of performance is basically considered while choosing any alcohol. Ethanol is easily produced from renewable agriculture resources, also it is and extraction solvent having high dissolving power for the oils so it is preferred over methanol for the transesterification of vegetable oils. Moreover the extra carbon atom present in the ethanol molecule gives a margin to increase the heat content and cetane number of the fuel produced [20].

1.2 Problem statement

Due to the lack of a well-developed, efficient and cost effective system for the production of biodiesel, it is still considered as an expensive alternative in comparison to petro diesel. This all happens due to the improper selection of raw material and catalyst for the process accompanied with other technological deficiencies and factors effecting the yield of biodiesel and its purity [21]. There is a variety of catalytic components which are utilized in the process classified as acids, alkalis, solid catalysts and enzymes [22].

Homogenous catalysts are relatively low in their activity due to soap formation which play a vital role in the inability to separate glycerol and purify fatty acid methyl ester (FAME) with water [23]. For raw materials with high FFA content strong acidic catalysts are preferable to be used because it will inhibit soap formation [24]. Heterogeneous solid catalyst are a convenient option for easy separation and reusability [25] with larger surface area to increase the active sites [24].

Metal organic frameworks (MOFs) are the emerging category of materials with wide range of applications in scientific research e.g., energy storage, catalytic activities, electrochemistry magnetism, drug delivery, adsorption and separation of gases and many other. They are porous solids with a well-structured assembly of coordinated bonds between their metal ions and organic ligands where a large number of synthesis approaches are being considered [26]. MOFs have large surface area and multiple sites for the catalytic application [27] making them a promising alternative to solid catalysts utilized for biodiesel production due to their easy separation and reusability which benefits their use in industrial scale [28]. Optimized synthesis of MOFs is considered as an important upfront in research and development which will not only unleash the utmost performance efficiency but also other approaches as cost and the sustainability of the environment [29].

Copper-based MOF is a stable option in perspective of thermal and chemical options with a large surface area, accessible metal ion sites and mild synthetic conditions [28]. Copper based MOFs efficiently oxidize alcohols as heterogeneous catalysts converting them into their corresponding products [30] hence it has been an efficient catalyst when used for biodiesel production [29].

The synthesis of carbonate based metal precursor is of importance due to its excess presence in mineral deposits. It has been experimented to be a versatile precursor having a coordinated structure with probable scope of growth [31] , advantages in process ability and clean reactivity.

1.3 Hypothesis

Synthesis of structured material can prove to be an efficient material for biodiesel production with improved catalytic activity. As structured materials e.g., metal organic framework will provide a larger surface area to carry on the reaction of biodiesel production which will enhance the rate of reaction and will result in improved percentage yield. Furthermore these materials being heterogeneous will help to avoid many other shortcoming which occur during the synthesis of biodiesel e.g. saponification, catalyst degradation and separation difficulties from the biodiesel sample [22].

1.4 Research objective

i. To synthesize and characterize Copper and Calcium based metal organic frameworks (MOFs) for biodiesel production

ii. To investigate the catalytic activity of Copper and Calcium based metal organic frameworks for esterification and transesterification

iii. To analyze the quality of the produced samples of biodiesel in accordance with the given standards.

1.5 Organizational structure and scope of study

The organizational structure of the study starts with the synthesis of synthesis of copper and calcium based metal organic frameworks (MOFs) which were then characterized using X-ray Diffraction (XRD), Scanning Electron Microscopy (SEM) and Thermo Gravimetric Analysis (TGA) techniques. These MOFs were then used as catalysts for the reaction of esterification and transesterification. Analysis of synthesized biodiesel samples was done by performing standard tests of pH, flashpoint, calorific value, Gas Chromatography Mass Spectroscopy (GCMS), Fourier Transform Infrared Spectroscopy (FTIR), iodine number, cetane number, saponification value, viscosity, density, specific gravity .

In this study copper and calcium based metal organic frameworks as catalysts are synthesized and studied for biodiesel production keeping in consideration the issues regarding production process like time, temperature and amount of catalyst required for the conversion of substrate (triglyceride / oil) into biodiesel (FAME). While the substrate studied here is waste cooking oil due to its availability, abundance, variant composition and high number of free fatty acid number which will enable to optimize the results with an even tricky substrate than using any unprocessed oil [21].

Summary

This chapter briefly discusses about the energy crisis in the country along with environmental problems caused by the use of fossil fuel resources. Waste cooking oil is a potential resource for biodiesel production which being a benign and renewable energy resource. Moreover the process of biodiesel production is briefly discussed along with the point of focus in this study which is the synthesis of a metal organic frameworks as a prospective catalysts for the production process.

References

[1] A. Herbst and C. Janiak, "MOF catalysts in biomass upgrading towards value-added fine chemicals," *CrystEngComm*, vol. 19, no. 29, pp. 4092–4117, 2017.

[2] Z. M. Hasib, J. Hossain, S. Biswas, and A. Islam, "Bio-Diesel from Mustard Oil : A Renewable Alternative Fuel for Small Diesel Engines," vol. 2011, no. November, pp. 77–83, 2011.

[3] F. U. M. Allah and G. Alexandru, "Waste cooking oil as source for renewable fuel in Romania," *IOP Conf. Ser. Mater. Sci. Eng.*, vol. 147, no. 1, 2016.

[4] T. Pangestu *et al.*, "The synthesis of biodiesel using copper based metal-organic framework as a catalyst," *J. Environ. Chem. Eng.*, vol. 7, no. 4, p. 103277, 2019.

[5] P. Collet, D. Spinelli, L. Lardon, A. Hélias, J. P. Steyer, and O. Bernard, "Life-Cycle Assessment of Microalgal-Based Biofuels," *Biofuels from Algae*, pp. 287–312, 2013.

[6] S. Silveira and D. Khatiwada, "Sugarcane Biofuel Production in Indonesia," in *Sugarcane Biofuels: Status, Potential, and Prospects of the Sweet Crop to Fuel the World*, M. T. Khan and I. A. Khan, Eds. Cham: Springer International Publishing, 2019, pp. 285–300.

[7] T. Ali, J. Huang, and J. Yang, "An Overview of Status and Policies on Biofuels in Pakistan," *Int. J. Econ. Res.*, vol. 3, no. 1, pp. 69–76, 2012.

[8] S. K. Sinha, K. A. Subramanian, H. M. Singh, V. V. Tyagi, and A. Mishra, "Progressive Trends in Bio-Fuel Policies in India: Targets and Implementation Strategy," *Biofuels*, vol. 10, no. 1, pp. 155–166, 2019.

[9] S. T. Coelho and J. Goldemberg, "Sustainability and Environmental Impacts of Sugarcane Biofuels," in *Sugarcane Biofuels: Status, Potential, and Prospects of the Sweet Crop to Fuel the World*, M. T. Khan and I. A. Khan, Eds. Cham: Springer International Publishing, 2019, pp. 409–444.

[10] S. D. Romano, P. A. Sorichetti, and G. Energy, "Introduction to Biodiesel Production," *Green Energy Technol.*, Springer, pp. 7–27, 2011.

[11] L. G. Pereira, O. Cavalett, A. Bonomi, Y. Zhang, E. Warner, and H. L. Chum, "Comparison of biofuel life-cycle GHG emissions assessment tools: The case studies of ethanol produced from sugarcane, corn, and wheat," *Renew. Sustain. Energy Rev.*, vol. 110, no. April, pp. 1–12, 2019.

[12] M. J. Borah, A. Das, V. Das, N. Bhuyan, and D. Deka, "Transesterification of waste cooking oil for biodiesel production catalyzed by Zn substituted waste egg shell derived CaO nanocatalyst," *Fuel*, vol. 242, no. January, pp. 345–354, 2019.

[13] M. José and A. L. Cardoso, "Heterogeneous Tin Catalysts Applied to the Esterification and Transesterification Reactions Production : A Brief Introduction," vol. 2013, 2013.

[14] Y. H. Tan, M. O. Abdullah, J. Kansedo, N. M. Mubarak, Y. S. Chan, and C. Nolasco-Hipolito, "Biodiesel production from used cooking oil using green solid catalyst derived from calcined fusion waste chicken and fish bones," *Renew. Energy*, vol. 139, no. November 2014, pp. 696–706, 2019.

[15] M. A. Raqeeb and R. Bhargavi, "Biodiesel production from waste cooking oil," vol. 7, no. 12, pp. 670–681, 2015.

[16] M. O. Abdullah and C. Nolasco-hipolito, "review," no. September 2018, 2019.

[17] S. A. Anand Kumar, G. Sakthinathan, R. Vignesh, J. Rajesh Banu, and A. H. Al-Muhtaseb, "Optimized transesterification reaction for efficient biodiesel production using Indian oil sardine fish as feedstock," *Fuel*, vol. 253, no. April, pp. 921–929, 2019.

[18] A. Talebian-kiakalaieh, N. Aishah, S. Amin, and H. Mazaheri, "A review on novel processes of biodiesel production from waste cooking oil," *Appl. Energy*, vol. 104, pp. 683–710, 2013.

[19] M. Su, R. Yang, and M. Li, "Biodiesel production from hempseed oil using alkaline earth metal oxides supporting copper oxide as bi-functional catalysts for transesterification and selective hydrogenation," *Fuel*, vol. 103, pp. 398–407, 2013.

[20] M. Chai, Q. Tu, M. Lu, and Y. J. Yang, "Esteri fi cation pretreatment of free fatty

acid in biodiesel production , from laboratory to industry," *Fuel Process. Technol.*, vol. 125, pp. 106–113, 2014.

[21] G. Knothe, "Biodiesel and renewable diesel : A comparison q," *Prog. Energy Combust. Sci.*, vol. 36, no. 3, pp. 364–373, 2010.

[22] L. T. Thanh, K. Okitsu, L. Van Boi, and Y. Maeda, "Catalytic Technologies for Biodiesel Fuel Production and Utilization of Glycerol: A Review," pp. 191–222, 2012.

[23] P. Sivakumar, K. Anbarasu, and S. Renganathan, "Bio-diesel production by alkali catalyzed transesterification of dairy waste scum," *Fuel*, vol. 90, no. 1, pp. 147–151, 2011.

[24] A. P. S. Chouhan and A. K. Sarma, "Modern heterogeneous catalysts for biodiesel production: A comprehensive review," *Renew. Sustain. Energy Rev.*, vol. 15, no. 9, pp. 4378–4399, 2011.

[25] C. Perego and A. Bosetti, "Microporous and Mesoporous Materials Biomass to fuels : The role of zeolite and mesoporous materials q," *Microporous Mesoporous Mater.*, vol. 144, no. 1–3, pp. 28–39, 2011.

[26] M. Sohail *et al.*, "Synthesis of Highly Crystalline NH -MIL-125 (Ti) with S-Shaped Water Isotherms for Adsorption Heat Transformation," vol. 125, 2017.

[27] Y. Fu, L. Sun, H. Yang, L. Xu, F. Zhang, and W. Zhu, "Visible-light-induced aerobic photocatalytic oxidation of aromatic alcohols to aldehydes over Ni-doped NH 2 -MIL-125 (Ti)," *"Applied Catal. B, Environ.*, vol. 125, 2016.

[28] G. Wu *et al.*, "Magnetic copper-based metal organic framework as an effective and recyclable adsorbent for removal of two fluoroquinolone antibiotics from aqueous solutions," *J. Colloid Interface Sci.*, vol. *528*, pp. 360-371, 2018.

[29] L. Chen *et al.*, "Biodiesel production over copper vanadium phosphate," *Energy*, vol. 36, no. 1, pp. 175–180, 2011.

[30] A. Taher, D. W. Kim, and I. M. Lee, "Highly efficient metal organic framework

(MOF)-based copper catalysts for the base-free aerobic oxidation of various alcohols," *RSC Adv.*, vol. 7, no. 29, pp. 17806–17812, 2017.

[31] D. Skala, "Calcium oxide based catalysts for biodiesel production : a review," vol. 22, no. 4, pp. 391–408, 2016.

Chapter 2

Literature review

2.1 Biodiesel overview

The energy demands is calculated to manifold by three times until 2050 as per evaluation though the supply or production side does not seem to be very progressive and reliable though the concerns are definitely required to intend towards energy production from alternative renewable resources. The current perspective of research in the field of biodiesel production targets on the production of biofuels as second generation with substrates like non edible plants /foods and waste vegetable oil. GOP discharged the tax and custom duty charges from the import of any utility required for biodiesel production such as plant, machinery, equipment and other items to help Economic Coordination Committee (ECC) of the cabinet to execute their decision of research and development in this field. Pakistan State Oil (PSO) company started its working to meet the deadline of 10% share of biodiesel by 2025 for which it selected non-edible plants/seeds species, such as castor, Jatropha, jojoba etc., for production of biodiesel. In Pakistan, the Alternative Energy Development Board (AEDB) also launched biofuel initiatives [7].

Pakistan is a rich land full of natural species and agricultural equity where 70% population works in farm fields and the soil survey classified into 79 types of soil throughout the country. More than 80 million acres of land which is of deprived quality and is best for cultivation of energy crops in Pakistan so this is a practical consideration for bioenergy production. Alcohol is also required for the production of biodiesel which is abundantly derived from sugarcane and synthesis of natural gas. The ultimate drawback of biodiesel technology as a potential candidate for renewable energy is the absence of awareness, education and collaboration between institutions. The 60% population located in rural areas utilize conventional methods like woods and organic waste (animal and crop residue) for domestic needs as they are unable to access commercial energy.

Hence progress in the field of bioenergy is required to fulfill the country's energy requirement to a momentous level. Moreover the emissions from diesel have around 79% highly toxic pollutants including inorganic and organic components which are not only dangerous for the environment (global warming, greenhouse gas emissions and smog formation) but for the health being carcinogenic and mutagenic such as sulfur oxide, nitrogen oxide and particulate matter [32].

Almost 21 distillery units around the country sufficient to process around 2 million tons of the molasses producing 400,000 tons of bioethanol are the main source of alcohol production from sugar cane though it exceeds the country's needs plus export by 318,000 tons. Thus we have sufficiently excess stock of alcohol for the process of transesterification for biodiesel production. Although methanol is more often used for this process because of its low price. Pakistan has the production capacity of 56 million tons of biodiesel after cultivating all the uncultured land around while the current requirement is nearly 8.5 million tons though a 10% increase of energy is expected per year. Hence biodiesel has an encouraging future in Pakistan due to the availability of raw materials and certain energy generation programs [33].

2.2 Biodiesel production

Biodiesel is an easily degradable and nontoxic fuel, free of exhaust gases in comparison to comparison to conventional diesel fuel. The esterification and transesterification reactions from vegetable oils or animal fats in the presence of alcohols and acid base catalyst are implied for biodiesel production. There is a wide range of homogenous and heterogeneous catalysts which is utilized for the synthesis of biodiesel such as acidic, basic or enzymatic etc. [34]. Chemically, molecules of biodiesel are mono-alkyl esters generally generated from esters of triglycerides.

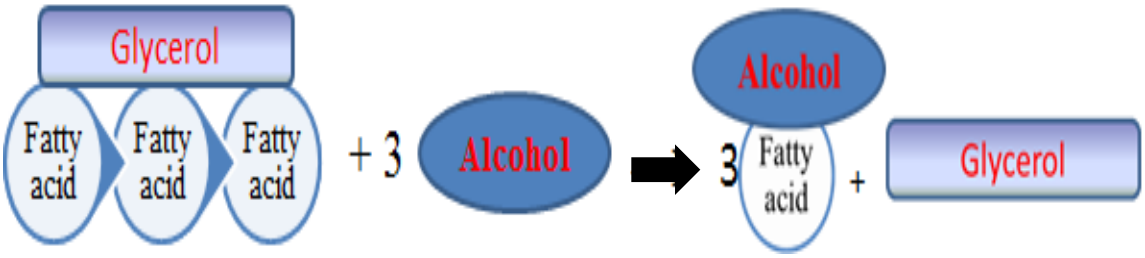

Figure 1 Standard chemical reaction mechanism of biodiesel production

In particular, there are three transesterification systems based on vegetable oil or animal fat, they are homogeneous, heterogeneous and enzymatic systems depending on the catalyst used in the method. UVO is reacted with alcohol, due to improved effectiveness, methanol is used in most instances. Ethanol and isopropyl alcohol, however, can also be used in animal fats [35].

There are several parameters on which the process of transesterification hinge on to have an optimized conversion which includes the properties of the substrate oil like moisture and FFA content or other physical and chemical properties, duration of reaction, rate of agitation or stirring, pressure, temperature, type of alcohol, molar ratio of alcohol to oil, type of catalyst and its quantity. The yield and purity of the product depend on all these parameters. The reaction temperature in this process plays an important role and usually set closer to the boiling point of alcohol. A number of studies discussed the reaction temperature to be maintained around 60 °C – 80 °C with an alcohol to oil molar ratio of 6:1. This molar ratio of alcohol to oil is also an effective parameter though this varies with type of catalyst and other factors in the reaction [36].

Table 1 discusses different researches carried out to produce biodiesel using waste cooking oil as a substrate. The studies show that waste cooking oil is proved to be a potential catalyst for biodiesel production with an approximate yield of 90 % using several acidic and basic catalysts.

Waste cooking oil, otherwise discarded is one of the most cost-effective biodiesel options. Since feedstock prices are one of the main issues about biodiesel production, the use of waste cooking oil considerably improves biodiesel production's financial viability. Since big amounts of waste cooking oil are illegally dumped into waterways and landfills, causing environmental pollution, the use of waste cooking oil to generate biodiesel as a petro diesel replacement provides important benefits owing to pollution decrease [2]. The production of biodiesel from waste cooking oils for diesel substitutes is particularly crucial due to the declining trend in global oil reserves, environmental issues created by the use of fossil fuel and the high price of petroleum products on the global market. Because of its elevated viscosity, there are several issues with the use of unprocessed vegetable oils in the ignition compression motors. The general method for the preparation of biodiesel is performed through a reaction between oil and alcohol in the presence of a catalyst called

Table 1 Researches carried out to convert waste cooking oil into biodiesel

Type/source of Oil	Catalyst	Reaction temp. (°C)	Oil to Alcohol ratio	Yield (%)	Conclusion	Ref.
Food factory	NaOH	60	-	68-70	All the five tested parameters complied with the ASTM criteria for fuel specifications.	[37]
Canola WCO	NaOH	60	1:3	94	Fourteen out of eighteen tested variables met the ASTM principles for fuel standards.	[38]
WCO	KOH	40	1 : 6	99.5	Highest yield of 99.5 % under optimum conditions from both feed stocks.	[39]
Cottonseed WCO	Lipase	64	1:3	-	Optimum reactant ratio was 3, where the observed reaction rate was maximum.	[40]
WCO	NaOH	60	1 : 7	87	A conversion yield of 87 % was achieved.	[41]
WCO	NaOH	70	1 : 10	88.6	The density of the biodiesel product was high energy which could be compared with fossil fuel based hydrocarbon.	[42]
WCO	BaO and KOH	80	1: 6	92	Less than 10% of energy is consumed during microwave heating method than the traditional one.	[43]
Mix of pig fat oil and WCO	NaOH	65	1:4	80	Optimized process parameters led to the maximum yield of 80 % by volume.	[44]
WCO	CZO	55	1:8	97.71	The catalyst due to its large surface area was reused for 5 cycles resulting in increased yield.	[45]
WCO	Ce- Mg/Al_2O_3	60	1:6	97	Ceria cobalt used less amount of catalyst than ceria magnesium to obtain more yield of conversion due to its high surface area and fast activity.	[46]
WCO	KOH	66.5	1:6.18	92.76	The optimum condition of biodiesel production were obtained at 1 wt.% KOH.	[36]
WCO	HCl, H_2SO_4, H_3PO_4 KOH	50	1:2.5	94	Alkali catalyst for transesterification of WCO proved to be an efficient catalyst.	[47]

transesterification. While in case of waste cooking oil as substrate it has large number of free fatty acid content hence esterification is performed prior to the step of transesterification. Both of these reactions require catalysts to speed up the reaction in the presence of alcohol [48].

2.3 Current status of catalyst application for biodiesel production

A lot of research work has been going on for the synthesis of catalytic material to enhance the process efficiency of any reaction [3]. Catalyst is the substance that accelerates a chemical reaction without itself being affected. It will provide the sites for the reactants to be activated and interacted together. On the other hand heterogeneous catalyst are emerging to seek great attention due to their reusable and noncorrosive nature carrying out transesterification and esterification reaction having acid and base both. There are several reported examples of heterogeneous catalysts as metal oxides, mixed metal oxides, alkali doped metal oxides and transition metal oxides etc [49].

Due to the short comings regarding source of raw material for the biodiesel production, non-edible domain is gaining focus. Homogenous catalyst causes the problem of intoxication and saponification during the conversion of Chinese tallow seed such as KOH, NaOH and CH_3ONa, due to higher acid value than rapeseed oil and soybean oil. The conversion of Chinese tallow seed oil by using acid-tolerant solid base catalyst to biodiesel. KF/CaO nanocatalyst synthesized through impregnation method showed 96.8 % biodiesel yield potential for industry use. Several countries like Germany, France, Italy, USA, Japan and so on are utilizing large amount of biodiesel. The green approach of heterogeneous catalyst use is introduced for the preparation of biodiesel which are occasionally mass transfer resistant, time consuming and inefficient. The limited applications for industry intrigue more focused research in this domain Biodiesel can also be known as environmentally benign fuel. An easier transesterification process for palm tree oil was carried out with help of TiO_2–ZnO nano catalyst which is a stable and active heterogeneous mixed metal oxide [50].

The developmental phase of biofuel energy largely depends upon catalytic reactions. Moreover, the integration of nanotechnology in the catalytic activity of biofuel production speeds up the process enhancing the product quality and amount of yield. The common problems caused by the use of heterogeneous catalysts e.g., mass transfer resistance, fast deactivation, time consumption and inefficiency; can be resolved by

replacing them with nano regime catalysts. The most demanded type of biofuel as biodiesel could be produced by nano catalysts which use nonedible feed substrate. The research done yet directs towards the fact that application of nanosized catalysts advances the production and efficiency rate of biofuel even at mild operation parameters with comparison to bulk catalysts [51].

Table 2 discusses different catalyst used for biodiesel production using a various substrates. Different studies are being carried out to produce biodiesel from variant substrates using NaOH, KOH and other metal composites as catalysts giving potential percentage yield.

2.4 Copper and calcium based catalyst for biodiesel production

Several studies have been done on the subject of biodiesel production using copper and calcium as catalysts. Table 3 gives a brief review of a few researches done in this regard.

Homogenous catalysts function at benign conditions with high reaction rate resulting in saponification and difficult separation of the product [62]. Heterogeneous catalysts are non-corrosive cheap, efficient in activity and environmental friendly. They do not produce waste water and are an artifact or continuous and economic process of biodiesel production. Metal oxides, inorganic acid salts and zeolites etc fall in this category. Many metal oxides are reported as active catalysts for the process of biodiesel production such as Ca, Mg, and Al while Cu based catalysts are rarely studied for this purpose. A study reported the synthesis of mesoporous structure of Cu-based supramolecular catalyst having a good catalytic activity for transesterification reaction [63]. A research found that the heterogeneous copper dopped zinc oxide nanocatalyst has enormous potential for biodiesel production from low-cost feedstock such as neem oil for viable energy manufacturing [61]. Bifunctional heterogeneous catalyst are gaining attention as they possess both acid and base to carry out the transesterification as well as esterification reactions [64].

Table 2 Different catalysts for biodiesel production from various substrates

Oil	Catalyst	Oil to alcohol ratio	Reaction temperature (°C)	Reaction time (mins)	Summary	Ref.
Crude castor oil	H_2SO_4 / KOH	1:4.5	60	120	Diesel engine performance and emission test on different Castor Biodiesel blends proved that it was suitable to be used as diesel blends with lower emission compared to conventional diesel.	[52]
Used Groundnut oil (UGO)	Cs-TPA/SBA1$_5$	1:6	60	120	A catalyst was synthesized to address the p[roblems of corrosion and reusability which gave a higher yield of 91.55.	[53]
Used vegetable oil	H_2SO_4	1:40	65	120	Optimization study showed that 1:19.8 oil to alcohol ratio worked to 15-25% FFA range while 55 sulfuric acid worked for 15-355 of FFA.	[20]
WCO	H_2SO_4/KOH	1:5	60	30	95.06% average biodiesel yield was achieved with WCO being a potential substrate.	[54]
WCO	Eggshell	1:9	85	165	Recycled eggshells used as catalyst for bidiesel production for diesel engine applications.	[55]
Neem Oil	NaOH	1:3	55-61	300	Biodiesel with all fuel properties lying within the standard range was produced.	[56]
Waste sunflower oil	NaOH	1:10	70	340	88.6% yield of biodiesel was obtained at 70°C temperature with 3.0% NaOH from waste sunflower oil, making it a viable alternative of fossil fuels.	[42]
Dairy waste scum as a feed stock	1.2 wt.% of Potassium Hydroxide	1:6	75	30	96.7% biodiesel yield was obtained from waste dairy scum.	[23]
WCO	KOH/NaOH	1:6	60	180	94.4% biodiesel with standard fuel properties was obtained using 0.4% KOH as catalyst.	[57]
Sunflower oil	Cs/Al/Fe3O4	1:14	58	120	94.8% biodiesel yield was obtained under optimal conditions.	[58]
Soybean oil	ZrO2 loaded with C4H4O6HK	1:16	60	120	98.03% yield was achieved with reusability of catalyst for five cycles.	[59]
Palm oil	TiO2-ZnO	1:12	60	300	98% yield was achieved with 200 mg catalyst loading under optimum reaction conditions.	[60]
Neem oil	CZO	1:10	55	60	97.18% yield was obtained while for the sixth catalyst reuse cycle 73.95% was achieved.	[61]

As already discussed, the step of transesterification is more efficiently done in the presence of base catalyst as acid catalyst hence it is generally experienced for the process of production of biodiesel [65]. The research focus considered here is to achieve the high number of active sites while using hetererogenous catalysts to improve the reaction mechanism and product output with special consideration to the certain limiting factors like saponification, reusability, ambient temperature and cost of the catalyst [66]. Ca based catalyst is one of the most studied systems for biodiesel production due to high activity, availability and its low cost [10]. A large number of researches related to the application of Ca based catalyst where it has shown varying conversion rates of oil into biodiesesel reaching to the record of 100 % [31].

Catalysts are commonly prepared using co-precipitation, solvothermal, sol-gel, impregnation, and hydrothermal Methods. Catalysts used in this study are copper and calcium based in the form of their metal organic frameworks (MOFs) synthesized by hydrothermal and solvothermal methods respectively. Copper based catalysts are rarely studied in general and not in MOF form while calcium based catalysts are already reported as efficient ones for biodiesel production but not much of the study is done for their MOF structure as well. Copper being acidic in nature will be used in the form of MOF to optimize the esterification reaction of the biodiesel production process while calcium being basic in nature will be used to work on the transesterification step. Table 3 shows Copper and Calcium based catalyst used for biodiesel production. Different metal composites are being synthesized to produce biodiesel from soyabean oil, hempseed oil, waste cooking oil, chineese tallow seed oil, neem oil and rubber seed oil etc.

2.5 Significance of operating conditions in biodiesel production

There are several operating conditions which are being monitored during the process of biodiesel production. Four basic factors which majorly impact the biodiesel production are discussed below such as alcohol to oil ratio, reaction time, reaction temperature and catalyst loading.

Table 3 Copper and calcium based catalyst used for biodiesel productio

Oil	Catalyst	Summary	Ref.
Hempseed oil	Cu/SrO	10% of the Cu/SrO presented a high catalytic performance for the process of tranesterifiation.	[19]
Soyabean oil	Cu/SrO	At optimum conditions of 65◦C temperature, 5h reaction time, 1:6.75 oil to alcohol ratio and 1.5 % catalyst loading, maximum conversion of soyabean oil into biodiesel.	[29]
WCO	CZO nanocomposite	97.71% biodiesel yield was obtained at optimum conditions being 50 min reaction time, 55◦C temperature, 1:8 oil to alcohol ratio and 12% catalyst loading.	[45]
Neem oil	CZO nanocatalyst	97.18% biodiesel yield was obtained at optimum conditions being 60 min reaction time, 55◦C temperature, 1:10 oil to alcohol ratio and 10% catalyst loading. While 73.95% of yield was achieved with catalyst re-used for sixth cycle.	[61]
Oleic acid	copper (II)-alginate	71.8% biodiesel yield was obtained at optimum conditions being 3h reaction time, 70◦C temperature, 1:10 oil to alcohol ratio and 250 mg catalyst loading.	[67]
WCO	calcium titanate (CT)	80.0 % biodiesel yield was obtained at optimum conditions being 60 min reaction time, 65◦C temperature, 1:15 oil to alcohol ratio and 1% catalyst loading.	[68]
Soyabean oil	Ni/Zn/Fe_2O_4 doped with Cu	Biodiesel yield was obtained using 10 g soya bean oil at optimum conditions being 2h reaction time, 160◦C temperature, 1:20 oil to alcohol ratio and 4% catalyst loading.	[69]
Xanthium sibiricum Patr oil	copper-based supramolecular (β-cyclodextrins)	88.63 % biodiesel yield was obtained at optimum conditions being 9h reaction time, 120◦C temperature, 1:40 oil to alcohol ratio and 8% catalyst loading.	[63]
rubber seed oil	(CuO/C)	Esterification reaction was performed at optimum conditions being 6h reaction time, 65◦C temperature, 1:10 oil to alcohol ratio and 8% catalyst loading.	[70]
WCO	Ca(OCH3)2	90.2% biodiesel yield was obtained at optimum conditions being 90 min reaction time, 65◦C temperature, 1:6 oil to alcohol ratio, 7000 rpm rotation and 4% catalyst loading.	[71]
Chinese tallow seed oil	KF/CaO nanocatalyst	96.8% biodiesel yield was obtained under optimum conditions.	[72]

2.5.1 Alcohol to oil ratio

The excess amount of alcohol during the biodiesel reaction process corresponds to the complete conversion of oils and fats into esters in a short time period. To ensure a complete transesterification reaction, the molar ratio of alcohol to triglycerides should be optimized to reach the suitable ratio. Theoretically, one mole of methanol is required for the esterification of one mole of FFA, however, excess amount of methanol results in enhanced FFA conversion [47]. Although alcohol has to removed or recovered from the biodiesel later on for product purification purposes [73] [74].

2.5.2 Reaction time

The conversion into esters is directly proportional to the increase in reaction time until it reaches to an optimum time period as per required for the specific substrate and catalyst type. Although the reaction time majorly depends upon the presence of reactants. The conversion rate of fatty acid esters increases with reaction time [75] while to have great yield with low production cost the reaction time must be optimized [3]. The rate of esterification generally increases with time but after a certain limit the activity becomes constant despite of the increase in time.

2.5.3 Reaction temperature

The increase in the reaction temperature decreases the viscosities of oils which results in a greater reaction rate in a shorter time period. While the temperature must be lower than the boiling point of the alcohol. Moreover after an optimal temperature, further increase starts the reaction of saponification. The step of esterification is found to be temperature specific. The optimal temperature ranged between 50 - 60 °C, depending on the oil used [34].

2.5.4 Catalyst loading

Catalyst loading can affect the yield of the biodiesel product. The increase in catalyst concentration directly correlates with the conversion rate of substrate into biodiesel. Furthermore an incomplete amount of catalyst results in the incomplete conversion of the triglycerides into fatty acid esters. The optimal condition of catalyst concentration is about 1.5 wt.% for NaOH which is the most commonly used catalyst [76]. There is a variety of catalytic components which are utilized in the process of transesterification such as carbonates, hydroxides and alkoxides classified as acids,

alkalis, solid catalysts and enzymes to produce around 10 million tons of biodiesel fuel from vegetable oil [22]. Catalyst choice mainly depends on the amount of FFA and raw materials in the oil for example oils having high water and FFA content will be preferably undergo transesterification with acidic catalysts with high temperatures (60-100 °C) and longer reaction time (2-10 h) along with corrosion of the equipment [22]. The concentration of right amount of catalyst can be maintained by performing optimization reactions for a certain type of substrate. Otherwise it could lead to incomplete reaction or saponification.

Summary

This chapter reviews the potential of biodiesel as a renewable energy source in Pakistan initially, then the current status of biodiesel production around the world and in Pakistan in specific reference to waste cooking oil. The second part of the review of literature covers the assessment of the current status of catalyst synthesis for biodiesel production in world and Pakistan accompanying the review of copper and calcium-based catalyst for biodiesel production. Due to the short comings regarding source of raw material for the biodiesel production, non-edible domain is gaining focus. For the commercial execution of transesterification process it is required to prepare cost effective heterogeneous catalysts as this is the limiting factor for their application in industrial use. The energy released from biomass is renewable and environmentally friendly, so it is strongly recommended to be applied while introducing nanotechnology research to biomass conversion has witnessed rapid growth. Metal organic frameworks have high specific surface and high catalysis activities, may solve the above problems. They have become the focus of recent research. Moreover, the factors effecting the biodiesel production are also discussed along with their significance.

References

[1] T. Ali, J. Huang, and J. Yang, "An Overview of Status and Policies on Biofuels in Pakistan," *Int. J. Econ. Res.*, vol. 3, no. 1, pp. 69–76, 2012.

[2] M. Ahmad, H. A. Jan, S. Sultana, and M. Zafar, "Prospects for the Production of Biodiesel in Pakistan Prospects for the Production of Biodiesel in Pakistan," no. September 2015, 2017.

[3] N. A. Khan and H. Dessouky, "Prospect of biodiesel in Pakistan," vol. 13, pp. 1576–1583, 2009.

[4] A. Gashaw and A. Teshita, "Production of biodiesel from waste cooking oil and factors affecting its formation: A review," *Int. J. Renew. Sustain. Energy*, vol. 3, no. 5, pp. 92–98, 2014.

[5] M. Abdul Raqeeb, "Biodiesel production from waste cooking oil," *J. Chem. Pharm. Res.*, vol. 7, no. 12, pp. 670–681, 2015.

[6] W. A. Kawentar and A. Budiman, "Synthesis of biodiesel from second-used cooking oil," *Energy Procedia*, vol. 32, pp. 190–199, 2013.

[7] N. H. Abdullah, S. H. Hasan, N. Rahmah, and M. Yusoff, "Biodiesel Production Based on Waste Cooking Oil (WCO)," vol. 1, no. 2, pp. 94–99, 2013.

[8] A. B. Chhetri, K. C. Watts, and M. R. Islam, "Waste Cooking Oil as an Alternate Feedstock for Biodiesel Production," *Energies*, vol. 1, no. 1, pp. 3–18, 2008.

[9] A. B. M. S. Hossain and A. N. Boyce, "Biodiesel production from waste sunflower cooking oil as an environmental recycling process and renewable energy," *Bulg. J. Agric. Sci.*, vol. 15, no. 4, pp. 312–317, 2009.

[10] D. M. Chesterfield, P. L. Rogers, E. O. Al-Zaini, and A. A. Adesina, "Production of biodiesel via ethanolysis of waste cooking oil using immobilised lipase," *Chem. Eng. J.*, vol. 207–208, pp. 701–710, 2012.

[11] S. C. S. Filhoa *et al.*, "The Potential of Biodiesel Production from Frying Oil Used in the Restaurants of São Paulo city , Brazil," *Chem. Eng. Trans.*, vol. 37, pp. 577–

582, 2014.

[12] B. A. Udeh, “Biodiesel Production from Waste Vegetable Oil (Sunflower) Obtained from Fried Chicken and Plantain,” vol. 8, no. 1, pp. 1–6, 2017.

[13] P. D. Patil, “Biodiesel Production from Waste Cooking Oil Using Sulfuric Acid and Microwave Irradiation Processes,” *J. Environ. Prot. (Irvine,. Calif).*, vol. 03, no. 01, pp. 107–113, 2012.

[14] S. P. K. and S. V. C. Math M. C, “Optimization of biodiesel production from oils and fats with high free fatty acids,” vol. 3, no. 3, pp. 318–321, 2010.

[15] B. Gurunathan and A. Ravi, “Biodiesel production from waste cooking oil using copper doped zinc oxide nanocomposite as heterogeneous catalyst,” *Bioresour. Technol.*, vol. 188, pp. 124–127, 2015.

[16] M. Abdelfatah, Y. Kiros, and A. E. R, “Petroleum & Petrochemical Engineering Journal Biodiesel Production from Waste Cooking Oil Using Different Heterogeneous Catalysts Support on Alumina,” pp. 1–7, 2017.

[17] Sahar *et al.*, “Biodiesel production from waste cooking oil: An efficient technique to convert waste into biodiesel,” *Sustain. Cities Soc.*, vol. 41, no. December 2017, pp. 220–226, 2018.

[18] C. O. Okpanachi, J. C. Chukwu, E. N. Yisa, H. Z. Abdullahi, and S. Sadiq, “Study Of The Physicochemical Analysis Of Biodiesel Produced From Waste Vegetable Oil .,” vol. 6, no. 07, pp. 6–8, 2017.

[19] T. S. Julianto and R. Nurlestari, “Waste cooking oil as source for renewable fuel in Romania Waste cooking oil as source for renewable fuel in Romania,” 2016.

[20] X. Chen, W. W. Qian, X. P. Lu, and P. F. Han, “Preparation of biodiesel catalysed by KF/CaO with ultrasound,” *Nat. Prod. Res.*, vol. 26, no. 13, pp. 1249–1256, 2012.

[21] A. C. C. Chang, R. F. Louh, D. Wong, J. Tseng, and Y. S. Lee, “Hydrogen production by aqueous-phase biomass reforming over carbon textile supported Pt-Ru bimetallic catalysts,” *Int. J. Hydrogen Energy*, vol. 36, no. 14, pp. 8794–8799,

2011.

[22] M. Ismail and M. Salim, “Biodiesel Production from Castor Oil and Its Application in Diesel Engine,” no. December 2014, 2018.

[23] A. Anitha, “Transesterification of Used Cooking Oils Catalyzed by CsTPA / SBA15 Catalyst System in Biodiesel production,” vol. 4, no. 1, pp. 5–8, 2012.

[24] M. Chai, Q. Tu, M. Lu, and Y. J. Yang, “Esteri fi cation pretreatment of free fatty acid in biodiesel production , from laboratory to industry,” *Fuel Process. Technol.*, vol. 125, pp. 106–113, 2014.

[25] O. Adepoju, T. F, and Olawale, “Acid-Catalyzed Esterification of Waste Cooking Oil with High FFA for Biodiesel Production,” vol. 21, pp. 80–86, 2014.

[26] Y. Peng, K. T. T. Amesho, C. Chen, S. Jhang, F. Chou, and Y. Lin, “Optimization of Biodiesel Production from Waste Cooking Oil Using Waste Eggshell as a Base Catalyst under a Microwave Heating System,” pp. 1–16, 2018.

[27] H. Ali, M. Mashud, and R. Rubel, “Biodiesel from Neem oil as an alternative fuel for Diesel engine,” *Procedia Eng.*, vol. 56, pp. 625–630, 2013.

[28] P. Sivakumar, K. Anbarasu, and S. Renganathan, “Bio-diesel production by alkali catalyzed transesterification of dairy waste scum,” *Fuel*, vol. 90, no. 1, pp. 147–151, 2011.

[29] ALI MOHAMMED SALEH and KAVITA KULKARNI, “Production of Biodiesel from Waste Cooking Oil by Transesterification,” *Ing. y Univ.*, vol. 19, no. 1, pp. 155–172, 2015.

[30] M. Feyzi, A. Hassankhani, and H. Reza, “Preparation and characterization of Cs / Al / Fe 3 O 4 nanocatalysts for biodiesel production,” *Energy Convers. Manag.*, vol. 71, pp. 62–68, 2013.

[31] F. Qiu, Y. Li, D. Yang, X. Li, and P. Sun, “Bioresource Technology Heterogeneous solid base nanocatalyst : Preparation , characterization and application in biodiesel production,” *Bioresour. Technol.*, vol. 102, no. 5, pp. 4150–4156, 2011.

[32] R. Madhuvilakku and S. Piraman, “Bioresource Technology Biodiesel synthesis by TiO 2 – ZnO mixed oxide nanocatalyst catalyzed palm oil transesterification process,” *Bioresour. Technol.*, vol. 150, pp. 55–59, 2013.

[33] B. Gurunathan and A. Ravi, “Process optimization and kinetics of biodiesel production from neem oil using copper doped zinc oxide heterogeneous nanocatalyst,” *Bioresour. Technol.*, vol. 190, pp. 424–428, 2015.

[34] R.-R. A. B. from used frying oil. Encinar JM, Gonzalez JF, “Variables affecting the yields and characteristics of the biodiesel.,” *Ind Eng Chem Res*, vol. 44, pp. 5491–9., 2005.

[35] F. Chang, C. Yan, and Q. Zhou, “Synthesis of a New Copper-Based Supramolecular Catalyst and Its Catalytic Performance for Biodiesel Production,” vol. 2018, pp. 1–8, 2018.

[36] A. K. Endalew, Y. Kiros, and R. Zanzi, “Heterogeneous catalysis for biodiesel production from Jatropha curcas oil (JCO),” *Energy*, vol. 36, no. 5, pp. 2693–2700, 2011.

[37] K. Ferdous, M. R. Uddin, M. R. Khan, and M. a. Islam, “Preparation of Biodiesel from Soybean Oil by Using Heterogeneous Catalyst,” *Int. J. Energy Environ.*, vol. 4, no. 2, pp. 243–252, 2013.

[38] G. Lourinho and P. Brito, “Advanced biodiesel production technologies: novel developments,” *Rev. Environ. Sci. Biotechnol.*, vol. 14, no. 2, pp. 287–316, 2015.

[39] D. Skala, “CALCIUM OXIDE BASED CATALYSTS FOR BIODIESEL PRODUCTION : A REVIEW,” vol. 22, no. 4, pp. 391–408, 2016.

[40] M. Su, R. Yang, and M. Li, “Biodiesel production from hempseed oil using alkaline earth metal oxides supporting copper oxide as bi-functional catalysts for transesterification and selective hydrogenation,” *Fuel*, vol. 103, pp. 398–407, 2013.

[41] L. Chen *et al.*, “Biodiesel production over copper vanadium phosphate,” *Energy*, vol. 36, no. 1, pp. 175–180, 2011.

[42] Q. Zhang *et al.*, "Biodiesel Production by Catalytic Esterification of Oleic Acid over Copper (II)– Alginate Complexes," *J. Oleo Sci.*, vol. 497, no. 5, pp. 491–497, 2017.

[43] N. Y. Yahya, N. Ngadi, N. S. Lani, and M. W. Ali, "Pilot evaluation of calcium titanate catalyst for biodiesel production from waste cooking oil," *Chem. Eng. Trans.*, vol. 56, pp. 595–600, 2017.

[44] J. Dantas, J. R. D. Santos, R. B. L. Cunha, R. H. G. A. Kiminami, and A. C. F. M. Costa, "Use of Ni-Zn ferrites doped with Cu as catalyst in the transesterification of soybean oil to methyl esters," *Mater. Res.*, vol. 16, no. 3, pp. 625–627, 2013.

[45] H. R. Ong, M. R. Khan, M. N. K. Chowdhury, A. Yousuf, and C. K. Cheng, "Synthesis and characterization of CuO/C catalyst for the esterification of free fatty acid in rubber seed oil," *Fuel*, vol. 120, pp. 195–201, 2014.

[46] M. Hsiao, S. Hou, J. Kuo, and P. Hsieh, "Optimized Conversion of Waste Cooking Oil to Biodiesel Using Calcium Methoxide as Catalyst under," 2018.

[47] L. Wen, Y. Wang, D. Lu, S. Hu, and H. Han, "Preparation of KF / CaO nanocatalyst and its application in biodiesel production from Chinese tallow seed oil," *Fuel*, vol. 89, no. 9, pp. 2267–2271, 2010.

[48] C. A. Guerrero, A. Guerrero-romero, and F. E. Sierra, "Biodiesel Production from Waste Cooking Oil," *Biodiesel*, pp. 23–44, 2010.

[49] F. H. Alhassan, U. Rashid, and Y. H. Taufiq-yap, "Optimization of simultaneous production of waste cooking oil based-biodiesel using iron-manganese doped zirconia-supported molybdenum oxide nanoparticles catalyst," vol. 033101, 2016.

[50] D. Y. C. Leung, X. Wu, and M. K. H. Leung, "A review on biodiesel production using catalyzed transesterification," *Appl. Energy*, vol. 87, no. 4, pp. 1083–1095, 2010.

[51] B. Thangaraj, P. R. Solomon, B. Muniyandi, S. Ranganathan, and L. Lin, "Catalysis in biodiesel production — a review," pp. 1–22, 2018.

[52] L. T. Thanh, K. Okitsu, L. Van Boi, and Y. Maeda, “Catalytic Technologies for Biodiesel Fuel Production and Utilization of Glycerol: A Review,” pp. 191–222, 2012.

Chapter 3

Materials and methods

Copper and calcium-based metal organic frameworks (MOFs) are synthesized in this study by solvothermal and hydrothermal method respectively. The prepared MOF materials are heterogeneous solid catalysts. After the characteristic analysis, these catalysts were then used for the esterification and transesterification of waste cooking oil and methanol.

3.1 Materials used for experimentation

Table 4 List of chemicals used in the synthesis of materials

Sr #	Name	Purity	Purpose
1	Methanol (MeOH)	99%	Material Synthesis and Purification
2	Dimethylformamide (DMF)	99%	Material Synthesis and Purification
3	Distilled Water (DW)	99%	Material Synthesis
4	Benzene-1, 4-dicarboxylic acid (BDC)	98%	Material Synthesis
5	Copper(II) sulfate pentahydrate ($CuSO_4.5H_2O$)	99%	Material Synthesis
6	Calcium carbonate ($CaCO_3$)	99%	Material Synthesis
7	Sulfuric acid (H_2SO_4)	98%	Material Synthesis
8	Potassium hydroxide (KOH)	85%	Material Synthesis

3.2 Material synthesis

3.2.1 Synthesis of copper based metal organic framework

The synthesis of copper based metal organic framework (Cu-MOF) was done by using solvothermal method [77]. The 1:1 ratio of the metal salt ($CuSO_4.5H_2O$) and Benzene-1, 4-dicarboxylic acid (BDC) were dissolved in distilled water and Dimethylformamide (DMF) respectively and after mixing together in beaker, it was kept on a hotplate with stirring at 85 °C for 24 hours [77]. Afterwards filtration was done to remove the extra solvent followed up by oven drying at 80 °C for 7-8 hours. Prior to its use in application process vacuum oven drying was also done at 80 °C for 3-4 hours to enhance the catalytic activity of the sample. Figure 2 represents the graphical sketch of the synthesis methodology.

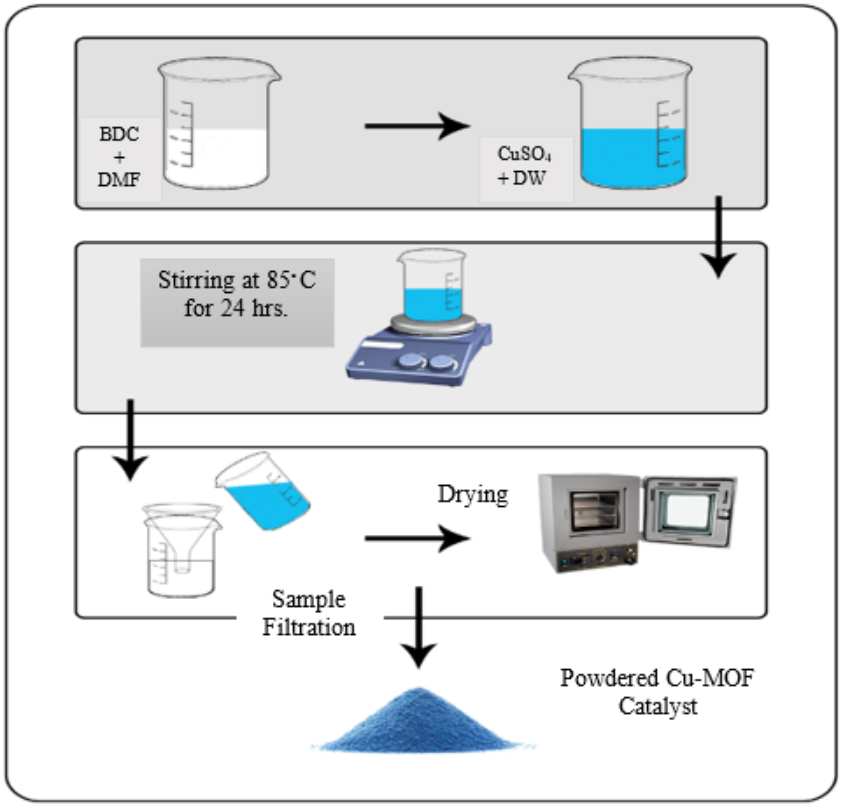

Figure 2 Graphical representation of the synthesis of Cu-MOF

3.2.2 Synthesis of calcium based metal organic framework

The synthesis of calcium based metal organic framework (Ca-MOF) was done by using hydrothermal method. The 1:1 ratio of the metal salt ($CaCO_3$) and Benzene-1,4-dicarboxylic acid (BDC) were dissolved in distilled water and Dimethylformamide (DMF) respectively and sealed in an autoclave, the sample was kept in the oven for 48 hours at 110 °C [78]. Afterwards filtration was done to remove the extra solvent followed up by oven drying at 80 °C for 7-8 hours. Prior to its use in application process vacuum oven drying was also done at 80 °C for 3-4 hours to enhance the catalytic activity of the sample.

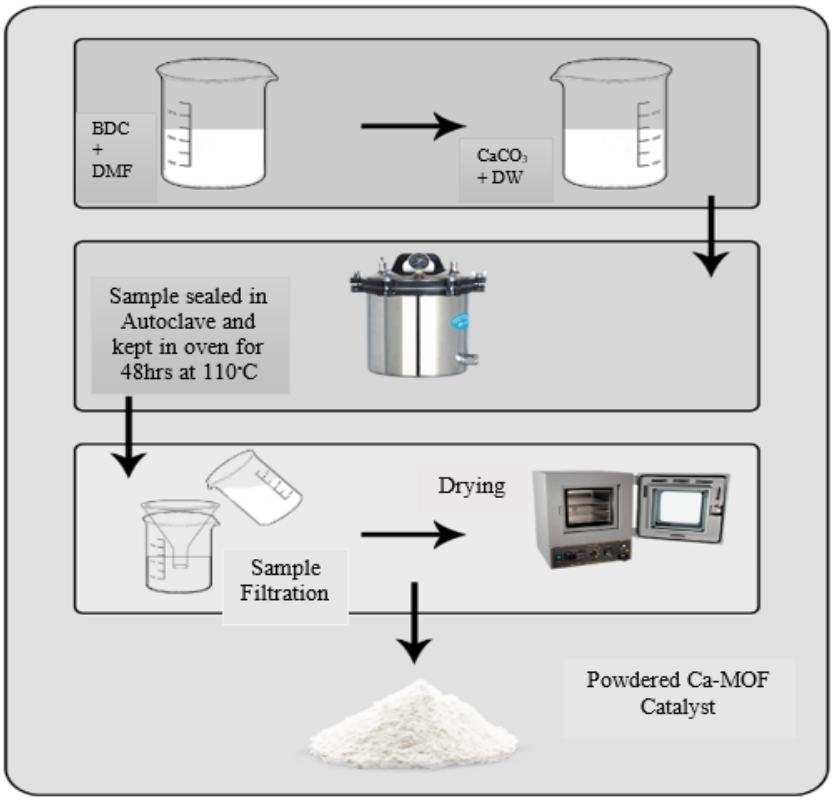

Figure 3 Graphical representation of the synthesis of Ca-MOF

3.3 Material characterization techniques

Research based on material synthesis highly requires characteristic analysis which is being done with the help of a number of characterization techniques available. This includes the examination of structure, elemental composition and other chemical or

physical properties which help in the accurate assessment of the sample to be used for further application process.

Crystal size, purity, dimensions of single unit, lattice parameters and other related information is obtained from X-ray diffractrometry (XRD) analysis. The XRD analysis was performed using Bruker's X-ray Diffractometer (D8 Advance) see supporting information in (Appendix 1, Figure S 1) connected with computer interface having Cu Kα at λ=1.5 Å.

The sample material was finely ground and kept on a well of plastic disc. All the XRDs were performed using 2θ value from 5 ° to 50 ° with a step of 0.05 ˚/min.

All the XRD patterns were analyzed using JADE software and peaks were identified through Search/match option with built in ICSD (Inorganic Crystal Structure Database) repository of software. The graphs were made on ORIGIN software. The output of an XRD scan is a spectrum with the y-axis being the intensity and x-axis is 2θ, where θ is the angle of incident X-rays on the sample. Certain peaks arise because of the phase shift of the diffracted X-ray due to the lattice spacing of the material.
The diffraction follows Bragg's law as shown in Equation 3.1:

$$\eta\lambda = 2d\sin\theta \tag{3.1}$$

The crystal size of the MOF particles was calculated using Scherer's Equation which is Equation 3.2.

$$D = \frac{0.9\lambda}{\beta\cos\theta} \tag{3.2}$$

Where n is an integer, λ the wavelength of the light, d is the spacing between crystal planes in the material, and θ is the angle of the incident light.

The morphology of the synthesized material was assessed taking its images using scanning electron microscopy (SEM). TESCAN VEGAN 3 was used to perform the SEM analysis (Appendix 1, Figure S 2). Powder samples were deposited on carbon tape fixed on a stage and was put inside the equipment. It was operated at 20 kV high voltage with secondary electron detector and tungsten detector type at angle of 45 °C. The lense of the

gun was lab-6. The sample SEM images were taken at three different magnifications of 2 µm, 5 µm and 10 µm.

To determine the thermal behavior of synthesized materials, TGA measurements were done using SHIMADZU-DTG 60H instrument (Appendix 1, Figure S 3). The thermograms were taken in continuous Nitrogen flow atmosphere (50ml/min) from 20 °C to 800 °C with sample held in alumina pan and weight loss against temperature plots were prepared for each sample. The temperature specifications of the sample for degradation at multiple steps were as for Pyrolysis: 80 – 120 °C, for Decomposition: 300 – 450 °C and for Combustion: > 450 °C.

3.4 Biodiesel production

3.4.1 Sampling of substrate waste cooking oil

The substrate waste cooking oil (WCO) was collected from locally. Oil was first filtered to remove any insoluble contaminations followed by heating it at 100 °C for moisture evaporation. Further the sample of WCO was stored at room temperature for biodiesel production reaction.

3.4.2 Pretreatment of waste cooking oil / esterification

The substrate oils having higher level of free fatty acid (FFA) content could undergo several side reactions in case of biodiesel production process hence its necessary to pretreat them. The substrate here in the research study is waste cooking oil (WCO) which has a higher FFA content and it was treated with acids also known as esterification before the process of transesterification in the presence of a base catalyst [52]. For esterification reaction, a 250 ml flask was mounted on a hotplate equipped with magnetic stirring reflux to ensure a uniformly agitated reaction mixture. The reaction contains 100 ml WCO, 20 ml methanol and 0.2 % acid catalyst. H_2SO_4 and Cu MOF catalyst were used for the esterification reactions, the prior for the standard sample and the later for the assessment of the catalytic activity of the synthesized catalyst. The reaction mixture was fed into the flask and experiment was conducted at 55 °C for 4 hrs. The sample was collected and centrifuged after the completion of reaction time. Methanol layer was separated and WCO was collected for further processing. The collected sample of WCO was washed with deionized water for three times followed by removal of water content by evaporation.

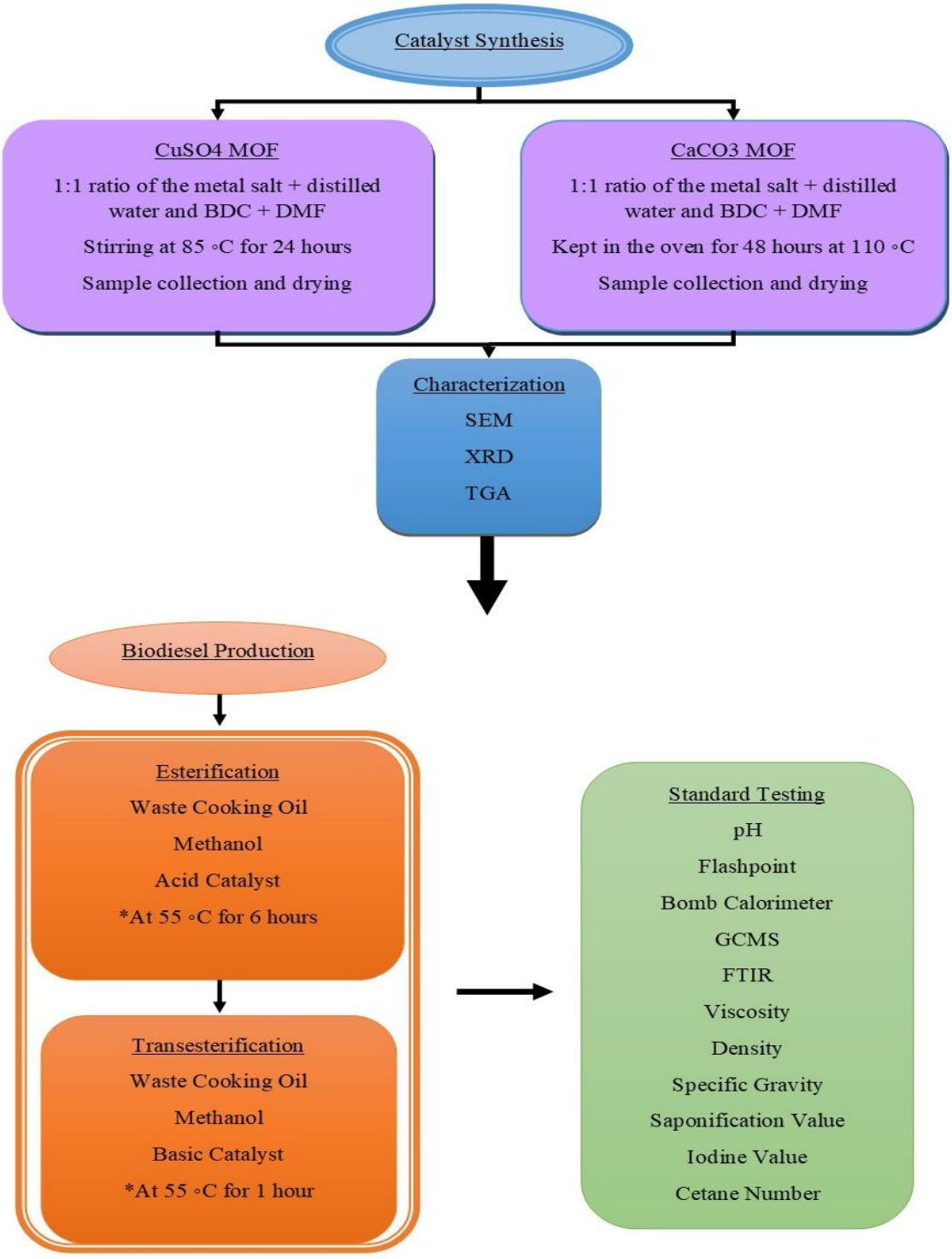

Figure 4 Graphical representation of the research methodology

At this point the FFAs values were calculated. Influencing parameters (methanol to oil ratio, catalyst dose, reaction time and temperature) were optimized and the FFA was calculated using the relation shown in Equation (3.3).

$$FFA \text{ conversion } (\%) = \left[\frac{A_i - A_t}{A_i} \times 100 \right] \tag{3.3}$$

Where, A_i and A_t, refer to the acidity (at time zero and t) [47].

3.4.3 Transesterification of pretreated WCO

KOH was mixed with methanol in a 250 ml flask mounted on a hotplate equipped with magnetic stirring reflux to ensure a uniformly agitated reaction mixture. The esterified oil was added in the flask and the reaction mixture was heated at 55 °C temperature with constant stirring for 1 h. Influencing parameters like methanol to oil ratio, catalyst dose, temperature and reaction time were optimized for biodiesel production process. After the reaction time was completed the sample was transferred into a separating funnel so that glycerol and biodiesel could be separated. Later biodiesel was washed with water in the ratio of 1:1 for several times. To remove unreacted catalyst and methanol. Excess water content was removed with evaporation and final sample of biodiesel was centrifuged at 4000 rpm for 10 min at room temperature and subjected to further characteristic analysis [53].

3.4.4 Experimentation inventory

For all the biodiesel production experimentation a two-step process was followed where for each experiment the first step of esterification was performed for 5-6 hours, while temperature and stirring rate was kept the same for both steps. Initially some feasibility experiments were performed with the standard catalysts and the two synthesized catalysts Cu-MOF and Ca-MOF. Later on a complete set of optimization reactions were performed with variant conditions to reach the maximum yield.

Table 5 Standard catalyst for biodiesel production (H_2SO_4 + KOH)

Feasibility Experiments						
#	**Catalyst (ml + g)**	**Oil (WCO) (ml)**	**Alcohol (MeOH) (ml)**	**Temperature (°C)**	**Stirring (rpm)**	**Reaction Time (min)**
1	2.5ml+ 1.5 g	100	20 + 25	53 - 55	600	60
2	12 ml + 6 g	500	100	54	600	60
3	1.25 ml + 1.25 g	50	10	55	600	60
4	2ml + 1.5 g	100	20	55	600	60
5	12 ml + 6g	500	100	54	600	60
Optimization Experiments						
	Catalyst (ml + g)	**Oil (WCO) (ml)**	**Alcohol (MeOH) (ml)**	**Temperature (°C)**	**Stirring (rpm)**	**Reaction Time (min)**
6	2.5 + 1	100	15	**50**	600	60
7	2.5 + 1	100	15	**55**	600	60
8	2.5 + 1	100	15	**60**	600	60
9	2.5 + 1	100	15	55	**400**	60
10	2.5 + 1	100	15	55	**600**	60
11	2.5 + 1	100	15	55	**800**	60
12	2.5 + 1	100	15	55	600	**60**
13	2.5 + 1	100	15	55	600	**90**
14	2.5 + 1	100	15	55	600	**120**
15	2.5 + 1	100	**15**	55	600	60
16	2.5 + 1	100	**18**	55	600	60
17	2.5 + 1	100	**20**	55	600	60

Table 6 Cu + KOH Catalyst for Biodiesel Production

Feasibility Experiments						
#	**Catalyst (g + g)**	**Oil (WCO) (ml)**	**Alcohol (MeOH) (ml)**	**Temperature (°C)**	**Stirring (rpm)**	**Reaction Time (min)**
1	1 + 1	100 + 100	15 + 20	53-55	600	60
2	1.5	96	30	60	800	120
3	1.5	96	30	60	600	90

4	0.5	32	10	60	600	60
5	1.5	96	30	65	400	60
6	0.5	32	10	60	600	60
7	0.75	75	13	55	550	60
8	1	100	15	55	550	60
9	1	100	18	55	600	120
10	1 + 0.5	100 + 50	18 + 10	53 + 55	600 + 600	180 + 60
			Optimization Experiments			
	Catalyst (g + g)	**Oil (WCO) (ml)**	**Alcohol (MeOH) (ml)**	**Temperature (°C)**	**Stirring (rpm)**	**Reaction Time (min)**
11	1 + 1	100	15	**50**	600	60
12	1 + 1	100	15	**55**	600	60
13	1 + 1	100	15	**60**	600	60
14	1 + 1	100	15	55	**400**	60
15	1 + 1	100	15	55	**600**	60
16	1 + 1	100	15	55	**800**	60
17	1 + 1	100	15	55	600	**60**
18	1 + 1	100	15	55	600	**90**
19	1 + 1	100	15	55	600	**120**
20	1 + 1	100	**15**	55	600	60
21	1 + 1	100	**18**	55	600	60
22	1 + 1	100	**20**	55	600	60
23	**1 + 1**	100	15	55	600	60
24	**1.5+1**	100	15	55	600	60
25	**2+1**	100	15	55	600	60

Table 7 H_2SO_4 + Ca Catalyst for Biodiesel Production

			Feasibility Experiments			
#	**Catalyst (ml + g)**	**Oil (WCO) (ml)**	**Alcohol (MeOH) (ml)**	**Temperature (°C)**	**Stirring (rpm)**	**Reaction Time (min)**
1	2.5 + 1	100+100	15+15	53 – 55	600	1-3 hr
2	0.5	50	50	50	400	60
3	0.75	62.5	12.5	55	500-600	1hr

4	1.8	150	30	50	400	60
	Optimization Experiments					
	Catalyst (ml + g)	**Oil (WCO) (ml)**	**Alcohol (MeOH) (ml)**	**Temperature (°C)**	**Stirring (rpm)**	**Reaction Time (min)**
5	2.5 + 1	100	15	**50**	600	60
6	2.5 + 1	100	15	**55**	600	60
7	2.5 + 1	100	15	**60**	600	60
8	2.5 + 1	100	15	55	**400**	60
9	2.5 + 1	100	15	55	**600**	60
10	2.5 + 1	100	15	55	**800**	60
11	2.5 + 1	100	15	55	600	**60**
12	2.5 + 1	100	15	55	600	**90**
13	2.5 + 1	100	15	55	600	**120**
14	2.5 + 1	100	**15**	55	600	60
15	2.5 + 1	100	**18**	55	600	60
16	2.5 + 1	100	**20**	55	600	60
17	**2.5 + 1**	100	15	55	600	60
18	**2.5+1.5**	100	15	55	600	60
19	**2.5+2**	100	15	55	600	60

Table 8 Standard Experimentation Details

#	Catalyst (g OR ml)		Oil (WCO) (ml)	Alcohol (MeOH) (ml)	Temperature (°C)	Stirring (rpm)	Reaction Time (min)
1	H_2SO_4 + KOH	2.5ml+ 1.5g	100	20 + 25	53 - 55	600	60
2	Cu-MOF+ KOH	1 g + 1 g	100	15 + 20	53-55	600	60
3	H_2SO_4+Ca-MOF	2.5 ml+ 1g	100	15+15	53 - 55	600	60
4	Cu-MOF + Ca-MOF	1 g + 1 g	100	20 + 20	53 - 55	600	60

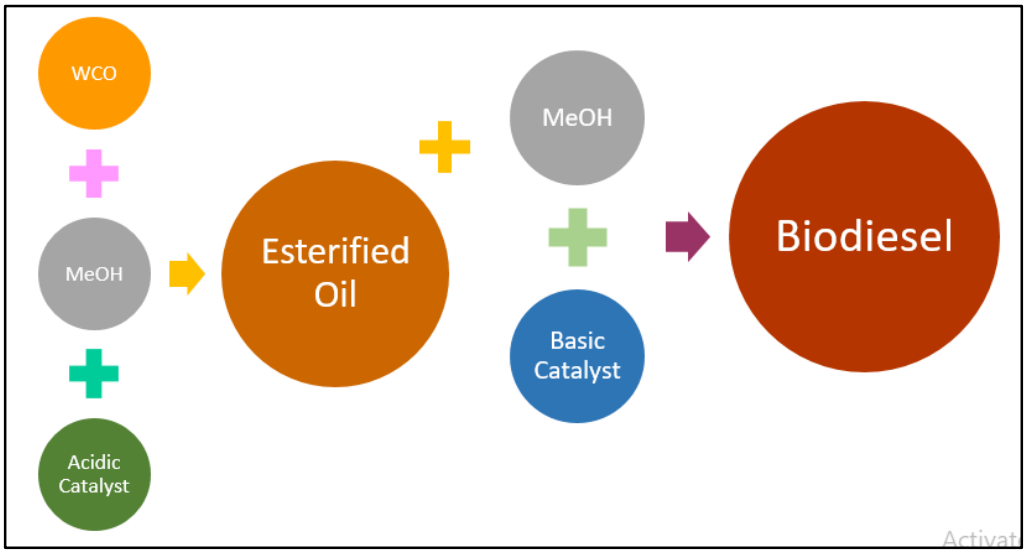

Figure 5 Generic Sketch of the Biodiesel Production Process

3.5 Biodiesel characterization

Several biodiesel characterization techniques were used to assess if the synthesized biodiesel samples are lying in the standard range. The analysis techniques used here in this study are pH, flashpoint, caloric value, GCMS, FTIR, viscosity, density, specific gravity, saponification value, iodine value and cetane number.

The pH of the biodiesel was determined by pH measuring strips while three calibration tests were performed to assure the results. Further for the purpose of cross verification the results were confirmed using HI9829 Multiparameter pH/ISE/EC/DO/Turbidity Waterproof Meter with optional GPS (Appendix 1, Figure S 4). With reference to a study controlling the pH at approximately 7.5 yielded quicker biomass accumulation and biodiesel production.

Flashpoint of any material is that lowest temperature which indicates its flammability in air hence the higher the flashpoint the safer and easily storable the biodiesel sample is [66]. The biodiesel samples in the study were tested for flashpoint using Seta flash Series 3 Active Cool Small Scale Flash Point Tester (Appendix 1, Figure S 5). Sample was fed into the inlet of the chamber where the flame was already lit with some gas supply.

The trend with which the biodiesel injection/supply effect the flame immediately at some specific temperature results with the flashpoint. The sample was tested at 80 °C, 110 °C and 140 °C to reach to the flashpoint of the sample.

The energy content of a sample determined by the complete combustion of a specific quantity which is expressed in joules per kilogram. 6200 Isoperibol Calorimeter (Appendix 1, Figure S 6) was used to analyze the calorific value of the prepared sample. 0.5 g weighed sample was kept in the 1108 Oxygen Combustion Bomb at intial temperature of 21°C with a rise of 2°C for further analysis which gave the calorific value of the sample [79].

The Shimadzu GCMS-QP2020 NX gas chromatograph-mass spectrometer (Appendix 1, Figure S 7) is used to determine the composition of fatty acid methyl esters (FAME) in the biodiesel sample. 25 mg of biodiesel sample was dissolved in 0.5 ml of n-hexane. The resulting sample solution is filled in GC auto sampler vial and injected in GC/MS to analyze and identify the fatty acid methyl ester composition. The injection volume was 1 µl with split ratio of 20:1 with initial set temperature of 150 °C and initial retention time of temperature was 5 minute. Maximum temperature of 220 °C with ramp of 10° /min with maximum retention time of 5 min. The inlet temperature was 250 °C and the detector transfer line temperature was 300 °C and the electron impact ion source mode was 70 eV. The scan range was 30-500 m/z where the ion source temperature was 200 °C and interface temperature of 250 °C.

Cary 630 FTIR Spectrometer (Appendix 1, Figure S 8) was used to analyze the absorption spectra of the samples. A small amount of sample was placed on the glass slide for the analysis in the wavelength range of 650-4000 cm^{-1}.

Viscosity is the fluid resistance to flow. The Brookfield Ametek DV2T Viscometer (Appendix 1, Figure S 9) was used to determine the viscosity at room temperature (~25 °C) at rpm of 50-150 where 2 ml of sample is required

The Density is the relationship between mass and volume of any substance hence calculated as mass per unit volume as in Equation (3.4).

$$\rho = \frac{m}{V} \tag{3.4}$$

A specific volume of the sample was taken and was weighed on the weighing balance to get the values of mass and volume so that its density can be calculated [80].

The value of specific gravity varies with the fatty acid composition and glycerin content in the sample. In reference to this a denser vegetable oil processes into a denser biodiesel which has high energy content and it results in increased power and better mileage. The specific gravity was calculated using the Equation 3.5.

$$\text{Specific Gravity} = \frac{\text{Density of Sample}}{\text{Density of Water}} \tag{3.5}$$

The saponification value (SV) is the amount of KOH (mg) required to saponify specific amount of biodiesel. It is reported that the pretreatment procedure of oil affects the saponification value. For the determination of saponification value, the 0.5 g biodiesel and 20 ml of 0.5 N alcoholic (ethanol) KOH was mixed. The mixture placed in round bottom flask, refluxed and heated at 40 °C until clear solution, an indicated of saponification reaction. After cooling the contents, phenolphthalein was added as indicator and mixture was titrated against 0.5 N HCl until the pink color disappeared. The saponification value was determined using relation shown in Equation 3.6.

$$SV = (B - S) \times N \times [\frac{56.1}{W}] \tag{3.6}$$

Where, B and S are the blank and sample values (HCl), N is normality of HCl and W is weight of biodiesel [47].

Iodine value (IV) measures the amount of iodine in g absorbed by 100 g oil. For the determination of iodine value, 0.1 g of biodiesel was mixed with 20 ml of CCl_4 and 25 ml Wijs reagent flask, shaken and placed the flask in dark for 30 min. Then, 20 ml of 15% KI was added in reaction mixture followed by the addition of 100 ml distilled water. Disappearance of yellow color indicated the end point. Same procedure was repeated for blank except the addition of biodiesel and iodine value was calculated using relation shown in Equation 3.7.

$$IV = \frac{[(B - S) \times N \times 12.69]}{W} \tag{3.7}$$

Where, B is the volume (ml) of 0.1 N $Na_2S_2O_3.5H_2O$ for blank, S is volume (ml) of 0.1 N $Na_2S_2O_3.5H_2O$ for sample (S), N is normality of $Na_2S_2O_3.5H_2O$ solution and W is weight of biodiesel.

The ignition quality of diesel depends on cetane number. Cetane number was calculated using the relation shown in Equation 3.8.

$$\text{Cetane Number} = 46.3 = [\frac{5458}{SV}] - 0.255 \times IV \tag{3.8}$$

The product yield is the percentage quantity obtained at the end of the experiment in comparison to the amount of reactants used for the biodiesel production process. This number tells about the extent of successful conversion of the substrate oil into biodiesel [47] as in Equation 3.9.

$$Yield\% = [\frac{\text{Amount of biodiesel produced}}{\text{Amount of oil}}] \times 100 \tag{3.9}$$

Summary:

This chapter discusses the experimental methodology implied to accomplish the goals of the study. The first part of the study involves the synthesis of copper and calcium based metal organic frameworks using solovo-thermal and hydrothermal synthesis methodologies respectively. Further the synthesized materials were characterized by using different techniques like SEM, XRD and TGA. The process of catalyst synthesis and working principal of characterization method is explained in this chapter. The second part of the study is biodiesel production involving esterification and transesterification reactions. Afterwards the biodiesel samples were analysed using characteristic analysis techniques as pH, flashpoint, calorific value, GCMS, FTIR, viscosity, density, specific gravity, saponification value, iodine value and cetane number. The results were assessed with the standard physical characteristic of biodiesel to analyze the quality of the product.

References

[1] J. Zhang, B. An, Y. Hong, Y. Meng, and X. Hu, "Pyrolysis of metal – organic frameworks to hierarchical porous Cu / Zn-nanoparticle @ carbon materials for efficient CO 2 hydrogenation †," pp. 2405–2409, 2017.

[2] Matjaz Mazaj and Natasa Zabukovec Logar, "Phase Formation Study of Ca-Terephthalate MOF-Type Materials," 2015.

[3] M. Ismail and M. Salim, "Biodiesel Production from Castor Oil and Its Application in Diesel Engine," no. December 2014, 2018.

[4] Sahar *et al.*, "Biodiesel production from waste cooking oil: An efficient technique to convert waste into biodiesel," *Sustain. Cities Soc.*, vol. 41, no. December 2017, pp. 220–226, 2018.

[5] A. Anitha, "Transesterification of Used Cooking Oils Catalyzed by CsTPA / SBA15 Catalyst System in Biodiesel production," vol. 4, no. 1, pp. 5–8, 2012.

[6] M. U. Kaisan *et al.*, "Calorific value , flash point and cetane number of biodiesel from cotton , jatropha and neem binary and multi-blends with diesel," *Biofuels*, vol. 0, no. 0, pp. 1–7, 2017.

[7] M. Ahmad, M. Zafar, S. Sultana, A. Azam, and M. A. Khan, "The optimization of biodiesel production from a novel source of wild non-edible oil yielding plant Silybum marianum," *Int. J. Green Energy*, vol. 11, no. 6, pp. 589–594, 2014.

Chapter 4

Results and discussion

4.1 Physical analysis of the synthesized catalyst

4.1.1 X-ray Diffraction (XRD) analysis

For the identification of the crystallography of synthesized catalysts, XRD was carried out. . Figure 6 and Table 9 shows XRD patterns with detail crystallinity of Cu-MOF and Ca-MOF after their synthesis through solvothermal and hydrothermal method respectively followed by vacuum drying.

A study represents the XRD pattern of the Cu(BDC) with sharp peaks which are in accordance with the synthesized MOF in the literature which confirmed that the synthesized sample was the desired Cu(BDC) metal–organic framework [81]. In another study the powder X-ray diffraction was measured to determine the crystallinity and purity of the sample where the data further confirms that there is no impurity in comparison with the JCPDS file of CuO, CuSO4 and Cu2O. [82] XRD patterns measured at 25 °C are in good agreement with their corresponding simulated patterns from the single-crystal data of Cu-MOF, which suggests that the phase purity of the bulk sample. The diffraction profiles of the sample remain until heating to 260 °C [83]. The following XRD pattern of the synthesized sample of copper MOF (Cu-MOF) shown in Figure 6 (a) tells that its characteristic peaks are in correspondence to the literature reviewed which confirms the successful synthesis of Cu-MOF.

The XRD patterns of simulated and synthesized Ca-BDC samples in previous studies done showed sharp peaks [78]. Where the characteristic peaks of the synthesized Ca MOF sample shown in Figure 6 (b) are in accordance with the reference peaks mentioned in the literature review so, the XRD results insure the successful synthesis of Ca-MOF.

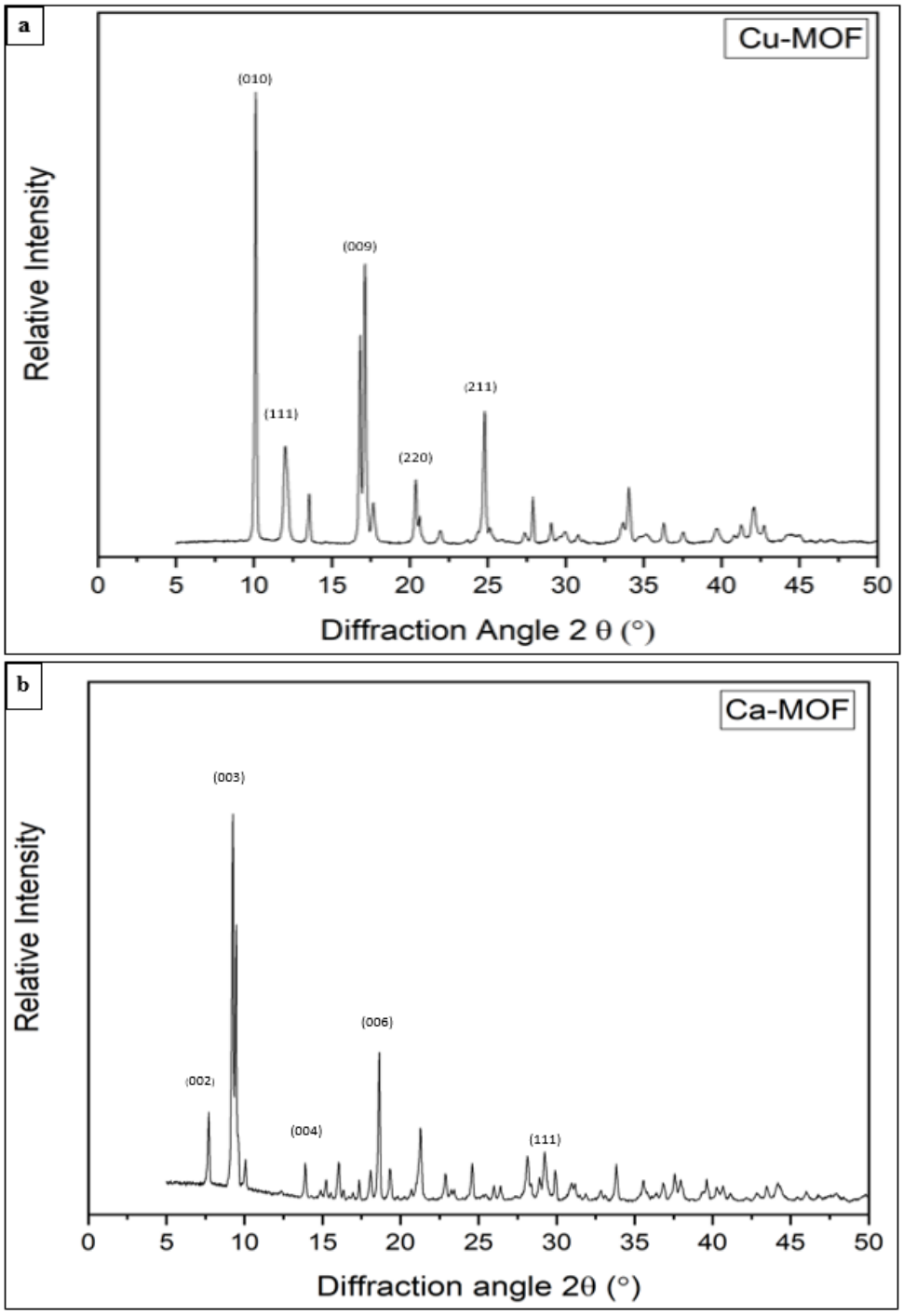

Figure 6 XRD Images of (a) Cu-MOF (b) Ca-MOF

The crystal size calculated using Scherer Equation was found to be 49.04 nm for Cu-MOF while 20.77 nm for Ca-MOF. Following Table 9 shows the XRD analysis along with crystallite size materials.

Table 9 XRD Analysis of Synthesized Cu-MOF and Ca-MOF

	2θ degree	**Space group**	**PDF #**	**hkl indices**	**d-spacing (nm)**	**Crystallite size (nm)**
Cu-MOF	17.146	Fm-3m (225)	74-2329	(009)	0.04	49.04
	12.073			(111)	0.07	32.67
	24.81			(211)	0.05	53.05
Ca-MOF	9.03	R-3m (166)	74-2328	(003)	0.2177	20.77
	18.63			(006)	0.038	66.52
	29.24			(111)	0.13	33.85

4.1.2 Scanning electron microscopy (SEM) analysis

The Cu-MOF synthesized here in this study revealed a highly crystalline cubical structure with an average size of 1-1.5 µm [82][84] as represented in Figure 7 studied at three different magnifications i.e. 2 µm, 5 µm and 10 µm. All the results of SEM images for Cu-MOF show varying shapes and sizes [28] [85]. While the one sample synthesized in this study showed rectangular sheets with well-defined crystallinity. The reason is stated as the difference in synthesis methodologies, reaction conditions and in some cases the application too for which they are being synthesized. The literature review showed the fact that the SEM analysis of copper based metal organic framework consist of irregular structures with varying shapes, some of them with high crystallinity.

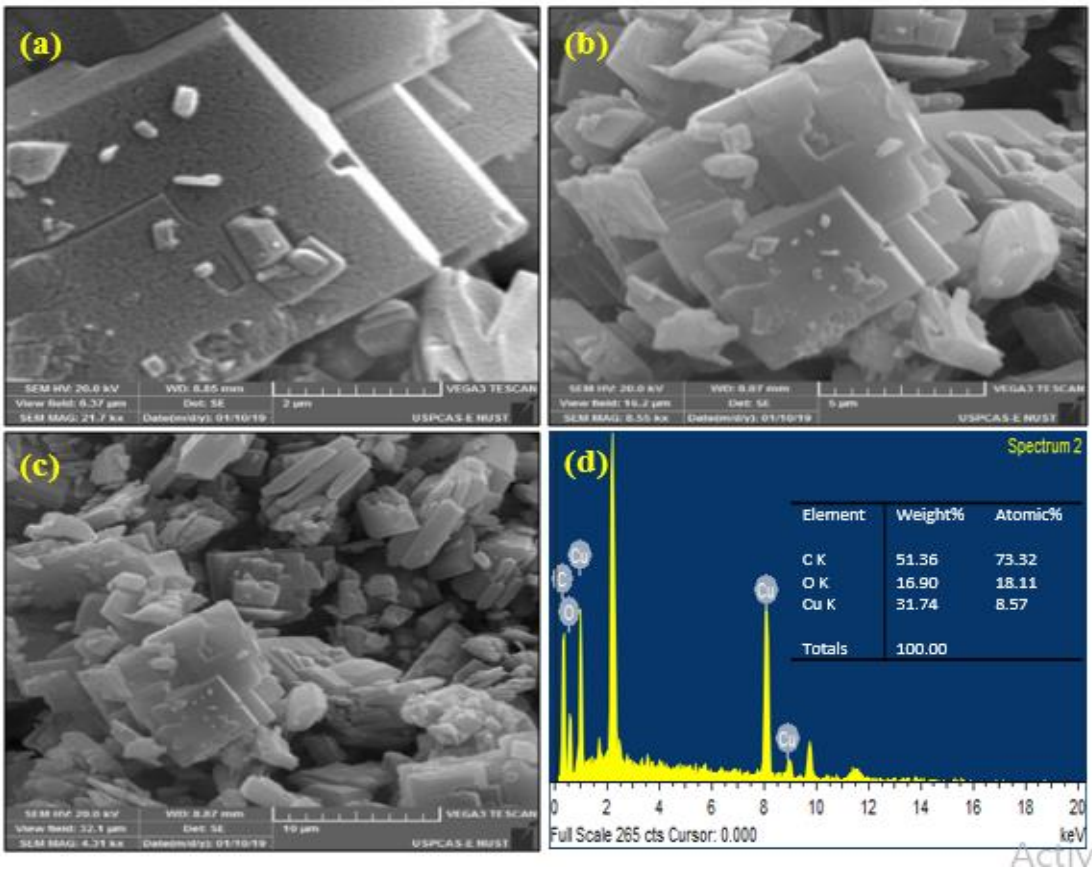

Figure 7 SEM Images of Cu-MOF at (a) 2µm (b) 5µm (c) 10µm (d) EDS with % weight of elements

The SEM images of synthesized Ca-MOF are shown in Figure 8 at three different magnifications i.e. 2 µm, 5 µm and 10 µm. These images showed that the Ca-MOF particles possess cubical shape with size of 2 µm. The small particles aggregated on the cubical particles are the unreacted contents which were later removed by washing. The Figure 8 (c) shows that there is presence of other shapes as well [78][86]. Literature review supported the results of the synthesized material. A study reported that the commercial CaO in irregular shape was still irregular even after treatment, but the morphologies became similar to each other, and the grains were sintered [87].

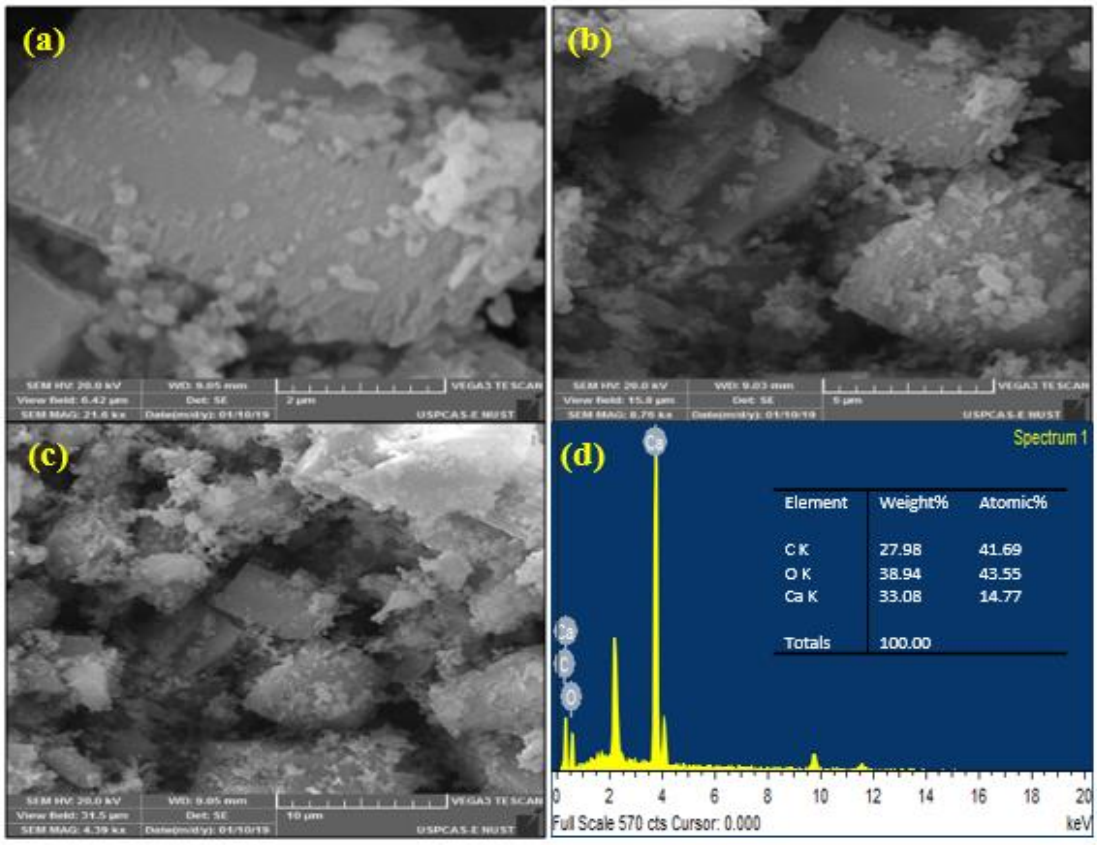

Figure 8 SEM Images of Ca-MOF at (a) 2µm (b) 5µm (c) 10µm (d) EDS with % weight of elements

4.1.3 Thermo gravimetric analysis (TGA)

In TGA although except mass, time and temperature as base measurements, many other additional measurements may be derived from these three. This provides information about the physical and chemical phenomenon such as phase transitions, absorption, and adsorption and desorption, chemisorption, thermal decomposition, and solid-gas reactions (e.g., oxidation or reduction).

The thermal stability or thermo gravimetric analysis of the copper MOF synthesized here was performed from 50-600 °C where the initial weight loss until 200 °C [83] was due to the evaporation or release of moisture content or DMF as shown in Figure 9 (a). According to the literature reference and the TGA analysis here the further weight loss is accompanied by the decomposition of organic linkers of the framework

which let to almost 35 % weight loss until 400 °C [82][83]. Further the weight loss almost remained constant with temperature rise until 600 °C [28][84].

The TGA analysis of the synthesized Ca-BDC showed the initial weight loss at 80 °C which is of DMF and water while that at 120 °C was Ca-BDC. Remaining DMF is removed from the materials upto 400 °C and further final degradation of Ca-BDC framework at 600 °C [78][86].

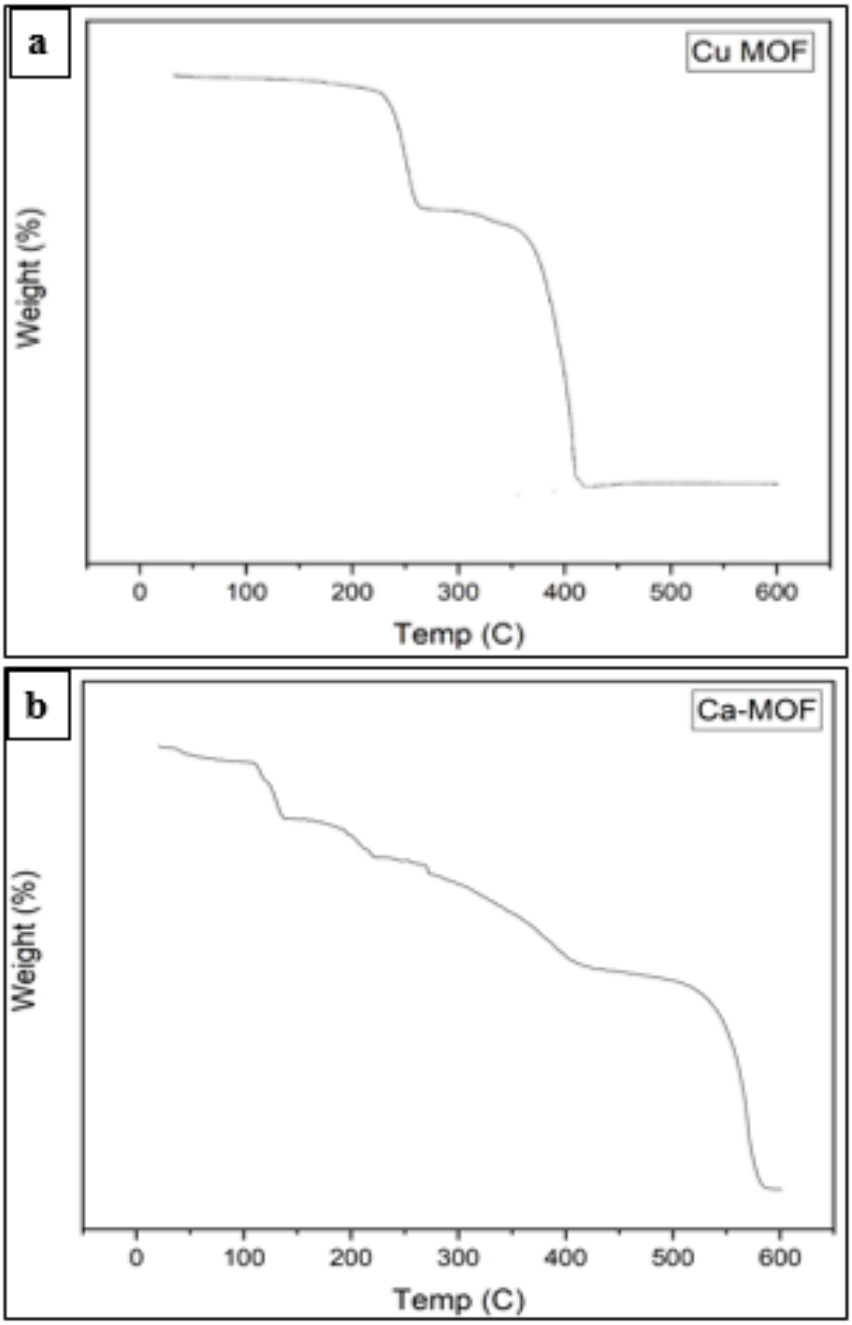

Figure 9 TGA Images of (a) Cu-MOF (b) Ca-MOF

4.2 Biodiesel analysis

4.2.1 Flashpoint

Flashpoint can be positively correlated with the viscosity of the diesel. The flashpoint is as higher as the boiling point and viscosity of the diesel. The lower molecular weight components of diesel lead to a reduced flashpoint [21] while higher flashpoints of biodiesel make it a reasonable alternative [88]. The standard value of flashpoint for biodiesel should be 130 °C or higher hence in case of Cu-MOF-BD it was 130 °C, for Ca-MOF-BD it was 140 °C and for Cu+Ca-MOF-BD it was 130.5 °C while the standard reference sample KOH-BD had 130 °C.

4.2.2 Calorific value

The calorific value of biofuels is an important parameter for the comparison of fuel properties with that of petroleum diesel [89]. The low energy contents of the biofuels affect the key performance parameters like maximum horsepower and torque [90]. The standard calorific value of biodiesel is around 37.27 MJ/kg while the difference in energy density of biodiesel samples dependent on the feedstock and production process could affect the calorific value. The calorific value of samples here was 40.07 MJ/kg for Cu-MOF-BD, 40.16 MJ/kg for Ca-MOF-BD and 40.37 MJ/kg for Cu+Ca-MOF-BD while the standard reference sample KOH-BD had a calorific value of 46.05 MJ/kg.

4.2.3 GCMS

The waste cooking oil is generated from the fried food. At high temperatures the composition changes along with organoleptic properties which affect both the food and oil quality. Reuse of oil may be harmful for because during recycling hazardous compounds are produced, which degrade the oil and food quality. So far, the alkali catalyzed process is a viable technique to convert WCO into biodiesel as and under the current issues of environmental pollution, there is a need to adopt renewable energy sources and green technique for energy generation [47].

The composition of WCO biodiesel determined in previous studies by using GCMS indicated the presence of methyl esters. From Gas Chromatography analysis, it was found that the biodiesel samples derived from waste cooking oil using KOH, Cu-MOF, Ca-MOF and both of these catalysts combined contains Oleic acid, Hexadecenoic

Table 10 GCMS Analysis of the Biodiesel Samples

KOH-BD GCMS		
Peak#	**Area%**	**Name**
61	0.17	7,10-Hexadecadienoic acid, methyl ester
62	0.25	7-Hexadecenoic acid, methyl ester
63	1.63	9-Hexadecenoic acid, methyl ester
64	0.26	9-Hexadecenoic acid, methyl ester
66	13.26	Pentadecanoic acid, 14-methyl-, m
78	28.29	9,12-Octadecadienoic acid (Z,Z)-,
79	26.64	9-Octadecenoic acid, methyl ester
81	0.29	Oleic Acid
82	0.29	9,12-Octadecadienoic acid (Z,Z)-,
83	0.18	.gamma.-Linolenic acid, methyl es
84	0.5	9,12,15-Octadecatrienoic acid, me
85	0.39	9,11-Octadecadienoic acid, methyl
86	0.17	9-Octadecenoic acid (Z)-, methyl e
87	0.11	8,11,14-Docosatrienoic acid, meth
88	0.18	10-Nonadecenoic acid, methyl este
89	0.43	Octasiloxane, 1,1,3,3,5,5,7,7,9,9,1
90	0.06	.gamma.-Linolenic acid, methyl es
92	0.07	cis-5,8,11-Eicosatrienoic acid, met
93	0.15	7,10,13-Eicosatrienoic acid, methy
94	0.37	.gamma.-Linolenic acid, methyl es
95	2.07	cis-11-Eicosenoic acid, methyl est
99	0.29	9-Octadecenoic acid
110	3.27	13-Docosenoic acid, methyl ester,
111	0.58	Docosanoic acid, methyl ester
119	0.23	Tricosanoic acid, methyl ester
137	0.39	Hexacosanoic acid, methyl ester

Cu-MOF-BD GCMS		
Peak#	**Area%**	**Name**
8	0.1	9-Hexadecenoic acid, methyl ester
9	1.47	9-Hexadecenoic acid, methyl ester
10	19.68	Hexadecanoic acid, methyl ester
14	0.11	Heptadecanoic acid, methyl ester
16	27.62	9,12-Octadecadienoic acid (Z,Z)-,
17	36.41	9-Octadecenoic acid, methyl ester,
18	2.7	11-Octadecenoic acid, methyl este
19	0.21	9,12,15-Octadecatrienoic acid, me
21	0.14	Oleic Acid
22	0.19	8,11-Octadecadienoic acid, methy
25	0.2	9,12-Octadecadienoic acid (Z,Z)-,
28	0.26	.gamma.-Linolenic acid, methyl es
31	0.24	.gamma.-Linolenic acid, methyl es
32	0.17	.gamma.-Linolenic acid, methyl es
33	0.1	cis-11,14-Eicosadienoic acid, met
41	0.26	Docosanoic acid, methyl ester
43	0.1	Tetracosanoic acid, methyl ester

Ca-MOF-BD GCMS		
Peak#	**Area%**	**Name**
100	0.34	Hexadecanoic acid, ethyl ester
106	0.21	9-Octadecenoic acid (Z)-, methyl ester
110	0.51	Oleic Acid
112	1.03	Linoleic acid ethyl ester
114	0.19	(E)-9-Octadecenoic acid ethyl ester
117	0.21	Octadecanoic acid, ethyl ester

acid, Linoleic acid, Octadecenoic acid and Octadecanoic acid. The rest others component acids indicated in each sample are listed in the Table 10.

4.2.4 FTIR

According to the literature reference the biodiesel from conventional diesel shows the alkane C-H bond on 2800 cm^{-1} to 3000 cm^{-1} wave number and alkene C–H bond at 1400 cm^{-1} to 1500 cm^{-1}. Biodiesel analysis also showed oxygen functional group of ester C–O bond at 1000 cm^{-1} to 1300 cm^{-1} and ester C=O bond at 1735 cm^{-1} to 1750 cm^{-1} shown in Figure 10. The presence of oxygen component in biodiesel provides cleaner and complete combustion unlike the conventional diesel [52].

As per prepared biodiesel samples with different catalysts like KOH-BD, Cu-MOF-BD and Ca-MOF-BD depict the same peaks of C-H and C-O bonds functional groups shown in Figure 10.

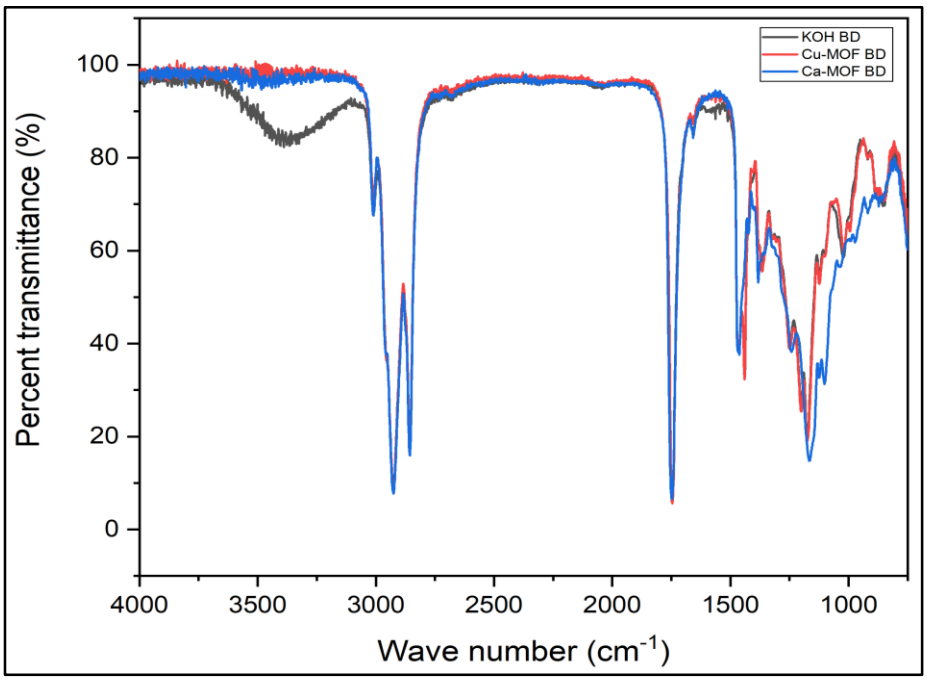

Figure 10 FTIR Spectrum of Synthesized Biodiesel Samples

4.2.5 Viscosity

The drop formation of biodiesel and quality of fuel air mixture combustion are dependent to the viscosity of fuel. Viscosity (very low/high) is undesirable for the proper

functioning of engine. Low viscosity leads to low penetration, which results in the black smoke emission due to low combustion.

A very viscous fuel may penetrate to the opposite wall of the injector, results in cold cylinder surface and leads to the low in combustion of fuel. The WCO biodiesel's viscosity was found to be 3.74, 5.72, 5.70 and 5.85 mm^2/s for KOH-BD, Cu-MOF-BD, Ca-MOF-BD and Cu+Ca-MOF-BD respectively. Which is within the standard range of 1.9–6.0 mm^2/s (ASTM D6751-02, 2002).

4.2.6 Density

The density of biodiesel significantly affects the engine performance. The density of biodiesel must be within the range to allow the optimized air fuel ratio for complete combustion in the engine. Diesel with high density value are not acceptable as it can lead to incomplete combustion and emission of particulate matter, but this problem could be solved by using blended biodiesel conventional diesel. The standard value of density for diesel is 848 kg/m^3 and for biodiesel is 870 kg/m^3– 900 kg/m^3 [88]. The density of biodiesel is around ~0.88 g/cm^3 (870 kg/m^3– 900 kg/m^3) which is higher than petro diesel. The density of WCO biodiesel calculated here as KOH-BD and Cu-MOF BD had density of 0.9 g/ cm^3, Ca-MOF-BD had 0.86 g/cm^3 and Cu+Ca-MOF-BD had 0.88 g/cm^3. The density of biodiesel was found to be 0.874 g/cm^3, which was within the range of fuel standard (ASTM standard).

4.2.7 Specific gravity

The specific gravity of biodiesel ranges from 0.86 to 0.90 where the standard reference sample KOH-BD and Cu-MOF-BD had specific gravity of 0.9, Ca-MOF-BD had 0.86 while Cu+Ca-MOF-BD had specific gravity of 0.88. The specific gravity of Biodiesel varies with its fatty acid composition, and its glycerin content, both free and bound. The same basic principles apply. A denser biodiesel has higher energy content and results in better mileage and increased power. Since the fatty acid content dictates the specific gravity, a denser vegetable oil processes into a denser biodiesel.

4.2.8 Saponification value

In combine effect of excess alcohol and KOH catalyst leads to saponification resulting in lower biodiesel yield and lower biodiesel quality [43]. The standard saponification value of biodiesel is < 312 mg KOH/g. The tested value of reference sample

KOH-BD here was 112.2 while that of Cu-MOF-BD was 252.45, Ca-MOF-BD was 193.35 and Cu+Ca-MOF-BD was 247.63. It is reported that the pretreatment procedure of oil affects the saponification value [47].

In the case of waste cooking oil containing high percentage of free fatty acid, alkaline catalyst reacts with free fatty acid and forms soap by saponification reaction. Also, it reduces the biodiesel conversions [91].

4.2.9 Iodine number

Iodine number is a measure of degree of unsaturation of biodiesel hence helpful to investigate the stability of oil. High degree of unsaturation results in polymerization of fuel due to epoxide formation due to addition of oxygen in double bonds. The standard value of iodine number for biodiesel should be < 120 g I_2 / 100 g oil. The iodine value of reference sample KOH-BD was 57.5 g I_2 / 100 g while that of Cu-MOF-BD was 60 g I_2 / 100 g, Ca-MOF-BD was 58.5 g I_2 / 100 g and Cu+Ca-MOF-BD was 61.32 g I_2 / 100 g.

4.2.10 Cetane number

The cetane number of biodiesel depends on the carbon number of fuel and FAME concentration. For biodiesel, the recommended range of cetane number is 46–52 and 40–55 for conventional diesel. The cetane number of reference sample KOH-BD was 50.5 while that of Cu-MOF-BD was 51, Ca-MOF-BD was 48.5 and Cu+Ca-MOF-BD was 52.

4.2.11 Product yield

The amount of biodiesel produced in correspondence to the amount of substrate used largely depends on the type of substrate, catalyst and other reaction conditions. Hence the results of product yield vary with the change in these reactants and reaction conditions. For the three different catalysts used the estimated product yield for biodiesel with standard catalyst (KOH-BD) was 98 %, biodiesel with Cu-MOF (Cu-MOF-BD) was 78.33 % and biodiesel with Ca-MOF was (Ca-MOF-BD) 78% while when both of the synthesized catalysts were used in a single chain of esterification and transesterification reaction the product yield was (Cu+Ca-MOF-BD) 85 %.

With reference to Table 8 having the details of the standard experiments following results in Table 11 are obtained from the characterization analysis done for the biodiesel samples produced.

Table 11 Fuel Properties of Biodiesel Produced from Waste Cooking Oil (WCO)

Properties	**Unit**	**BD standards**	**BD from WCO Ref.** [47]	**KOH-BD**	**Cu-MOF-BD**	**Ca-MOF-BD**	**Cu+Ca-MOF-BD**
Flashpoint	**°C**	>130		130	130	140	130.5
Specific gravity	**————**	0.86–0.9	0.8743	0.9	0.9	0.86	0.88
Viscosity	**mm^2/s**	1.9–6.0	5.83	3.74	5.72	5.70	5.85
Calorific value	**MJ/kg**	>35	37.2	46.048	40.068	40.16	40.37
Saponification value	**mg KOH/g**	<312	280	112.2	252.45	193.35	247.63
Iodine value	**g I_2/100g oil**	<120	63.5	57.5	60	58.5	61.32
Cetane number	**----**	≥47	51.48	50.5	51	48.5	52
Yield	**%**		94	98	78.33	78	85

The physical characteristics of the biodiesel sample are quite in accordance with the standard ranges showing improved results in comparison while the percentage yield is not as high as it could. Hence there is a window to work on the conversion and percentage yield by optimization of the reaction conditions.

Summary

This chapter includes the characteristic analysis of the synthesized Cu-MOF and Ca-MOF. The results of SEM, XRD and TGA are compared with the studies done in past, which are in accordance to each other. The results of biodiesel samples are also been compared with the standard values provided and lie in the given range.

The synthesized catalysts were characterized with SEM, XRD and TGA where the analysis results showed agreement with the literature review being done. XRD results showed sharp characteristics peaks while the crystal size calculated using Scherer Equation was found to be 49.04 nm for Cu-MOF while 20.77 nm for Ca-MOF. SEM images showed cubical images of 1.5 and 2µm for both Cu-MOF and Ca-MOF. TGA results showed that both the materials decomposed at 600° C.

The catalyst were then used for their application in the process of biodiesel production. Two separate reactions were performed for both the catalysts to produce the samples of biodiesel. Further several standard testing analysis techniques were used to compare the produced samples where the results were in agreement with the samples. Flashpoint of Cu-MOF-BD was 130 °C, Ca-MOF-BD was 140 °C while that of Cu+Ca-MOF-BD was 130 °C and calorific value of 40 kJ/g for each with a conversion of 78.33 %, 78 % and 85 % respectively.

References

[1] K. Huang, Y. Xu, L. Wang, and D. Wu, "RSC Advances Heterogeneous catalytic wet peroxide oxidation of simulated phenol wastewater by copper metal – organic frameworks," *RSC Adv.*, vol. 5, pp. 32795–32803, 2015.

[2] S. S. Menon, V. Chandran, and A. Koyappayil, "Copper- Based Metal-Organic Frameworks as Peroxidase Mimics Leading to Sensitive H 2 O 2 and Glucose Detection," pp. 8319–8324, 2018.

[3] W. Xu *et al.*, "Short communication A copper based metal-organic framework : Synthesis , modi fi cation and VOCs adsorption," *Inorg. Chem. Commun.*, vol. 92, pp. 1–4, 2018.

[4] Matjaz Mazaj and Natasa Zabukovec Logar, "Phase Formation Study of Ca-Terephthalate MOF-Type Materials," 2015.

[5] I. Ali, A. Badshah, M. Amtiaz, N. Haider, and M. Arif, "A copper based metal-organic framework as single source for the synthesis of electrode materials for high-performance supercapacitors and glucose sensing applications," *Int. J. Hydrogen Energy*, vol. 39, no. 34, pp. 19609–19620, 2014.

[6] J. Yang, F. Zhao, and B. Zeng, "One-step synthesis of a copper-based metal–organic framework–graphene nanocomposite with enhanced electrocatalytic activity," pp. 22060–22065, 2015.

[7] G. Wu *et al.*, "Magnetic copper-based metal organic framework as an effective and recyclable adsorbent for removal of two fluoroquinolone antibiotics from aqueous solutions," *J. Colloid Interface Sci.*, 2018.

[8] T. R. Fauziah, M. S. Sangi, and T. P. Oetami, "Calcium Oxide from Limestone as Solid Base Catalyst in Transesterification of Reutealis trisperma Oil," vol. 16, no. 2, pp. 208–213, 2016.

[9] Z. H. U. Huaping, W. U. Zongbin, C. Yuanxiong, Z. Ping, D. Shijie, and L. I. U. Xiaohua, "Preparation of Biodiesel Catalyzed by Solid Super Base of Calcium

Oxide and Its Refining Process," vol. 27, no. 5, pp. 391–396, 2006.

[10] G. Knothe, "Biodiesel and renewable diesel : A comparison q," *Prog. Energy Combust. Sci.*, vol. 36, no. 3, pp. 364–373, 2010.

[11] S. Ismail, S. A. Abu, R. Rezaur, and H. Sinin, "Biodiesel Production from Castor Oil and Its Application in Diesel Engine," vol. 31, no. 2, pp. 90–100, 2009.

[12] A. C. Drenth, D. B. Olsen, and K. Denef, "Fuel property quantification of triglyceride blends with an emphasis on industrial oilseeds camelina , carinata , and pennycress," *FUEL*, vol. 153, pp. 19–30, 2015.

[13] A. C. Drenth, D. B. Olsen, P. E. Cabot, and J. J. Johnson, "Compression ignition engine performance and emission evaluation of industrial oilseed biofuel feedstocks camelina , carinata , and pennycress across three fuel pathways," *FUEL*, vol. 136, pp. 143–155, 2014.

[14] Sahar *et al.*, "Biodiesel production from waste cooking oil: An efficient technique to convert waste into biodiesel," *Sustain. Cities Soc.*, vol. 41, no. December 2017, pp. 220–226, 2018.

[15] M. Ismail and M. Salim, "Biodiesel Production from Castor Oil and Its Application in Diesel Engine," no. December 2014, 2018.

[16] P. D. Patil, "Biodiesel Production from Waste Cooking Oil Using Sulfuric Acid and Microwave Irradiation Processes," *J. Environ. Prot. (Irvine,. Calif).*, vol. 03, no. 01, pp. 107–113, 2012.

[17] R. D. Saini, "Conversion of Waste Cooking Oil to Biodiesel," *Int. J. Pet. Sci. Technol.*, vol. 11, no. 1, pp. 9–21, 2017.

Chapter 5

Conclusions and future recommendations

5.1 Conclusion

- The study concluded with successful synthesis of Cu-MOF and Ca-MOF catalysts through solvothermal and hydrothermal processes respectively
- From the characterization through SEM, XRD and TGA the physical properties of the synthesized catalysts were analyzed. XRD results showed sharp characteristics peaks while the crystal size to be 49.04 nm for Cu-MOF while 20.77 nm for Ca-MOF. SEM images showed cubical images of 1.5 µm and 2 µm for both Cu-MOF and Ca-MOF respectively. TGA showed thermal stability of Cu-MOF until 400 °C and Ca-MOF until 520 °C.
- The synthesized catalysts were then used for biodiesel production where it ended up with 78.33 % product yield with Cu-MOF, 78 % with Ca-MOF and 85 % yield using Cu+Ca-MOF.
- Flashpoint of Cu-MOF-BD was 130 °C, Ca-MOF-BD was 140 °C while that of Cu+Ca-MOF-BD was 130.5 °C and calorific value of 40 MJ/kg for each of the sample. From GCMS analysis oleic acid, Hexadecenoic acid, Linoleic acid, Octadecenoic acid and Octadecanoic acid were found commonly in the all biodiesel samples.

5.2 Recommendations

- As the results show that the percentage yield of Ca-MOF-BD is lower than the Cu-MOF-BD hence there is a margin to work on this aspect. Future work could be aimed for the optimized production and increased percentage yield of the biodiesel using these catalysts.

- A comparative study could also be designed to assess the efficiency of these catalyst on other types of oils as catalyst for biodiesel production.
- The synthesis methodology of the catalyst largely effect the product which has the significant impact on the application hence optimized synthesis of Cu-MOF and Ca-MOF could be another research aspect to optimize for an efficient biodiesel production from them.
- To extrapolate this research to a commercial scale, proper development of production unit is required with monitored input of reactants and provision of temperature, stirring and separation.

Summary:

This chapter provides the concluding remarks for the study. Further needed work is also highlighted which is necessary for the achievement of the long term goal to optimize the process of biodiesel production considering various little but effective factors involved. For future perspective a rather efficient and augmented setup would play a significant role in the generation of biofuel.

Acknowledgments

All praise to the great Allah Almighty who made me the much capable that I could carry out this study and who enabled me to fulfill the obligation to explore the world of science up to my maximum limits.

I would like to express my sincere gratitude to my research supervisor Dr. Rabia Liaquat for her motivation, continuous support, patience and immense knowledge. She has guided me completely through-out my research work. I am also really thankful to my GEC members, Dr. Naseem Iqbal, Dr. Asif Hussain Khoja and Dr. Muhammad Bilal Sajid for sparing precious time from their busy schedules, for suggestions as well as moral support. It was an honor to be an exchange beneficiary and ambassador of Pakistan in Arizona State University, USA, so, I must be very thankful to USAID for giving me the opportunity to explore the American culture and academic system. A special thanks to lab engineers Ali Abdullah, Naveed Ahmad, Amin Durrani, Hassan Nazir, Asghar Ali and Qamar-ud-Din who helped me a lot in the experimental work and testing.

Last but not the least, I would pay my regards to my family especially my sister Samra Jamil, my brother Ahmad Hassan, my nieces Zoel Hassan and Raania Hassan for their kind encouragement. I would like to acknowledge the support of my friends who accompanied me in the lab work and motivated me to accomplish my goals Rida Mansoor, Rehan Anwar, Bushra Batool and M.Ali Qamar .

Appendix 1

Figure S 1 Bruker's X-ray Diffractometer (D8 Advance)

Figure S 2 Tescan Vegan 3 Scanning Electron Microscope

Figure S 3 SHIMADZU-DTG 60H Thermo gravimetric instrument

Figure S 4 pH Strips (on left), HI9829 Multiparameter pH/ISE/EC/DO/Turbidity Waterproof Meter with optional GPS (right)

Figure S 5 Seta flash Series 3 Active Cool Small Scale Flash Point Tester

Figure S 6 6200 Isoperibol Bomb Calorimeter

Figure S 7 Shimadzu gas chromatograph-mass spectrometer GCMS-QP2020 NX

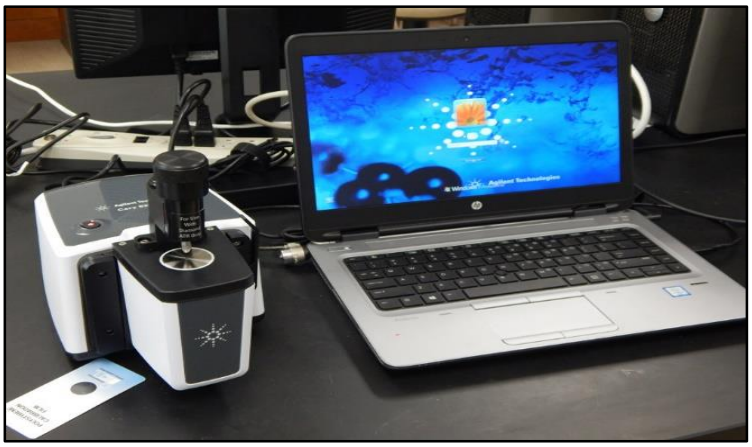

Figure S 8 Agilent Cary 630 FTIR

Figure S 9 Brookfield Ametek Dv2t Viscometer

Appendix 2

Photo catalytic Degradation of Organic Dyes by Semiconducting Metal Sulphide Nanoparticles of Copper and Zinc Synthesized through Single Source Precursor

Unza Jamil[a], Rida Mansoor[a], Bushra Batool[a], Rabia Liaquat [a*]

[a] U.S.-Pakistan Center for Advanced Studies in Energy, National University of Sciences & Technology Islamabad, Pakistan

[*] Corresponding Author E-mail: rabia@uspcase.nust.edu.pk

Abstract

Nanotechnology is emerging with novel applications in the current field of material science with nanoparticles and nanomaterials. The II-VI wide band-gap semiconducting metal sulphides are extensively used for the synthesis and characterization of their nanocrystals, having significant potential due to their optical and electronic properties. Zinc sulphide (ZnS) and copper sulphide (CuS) have been extensively studied in this regard. The synthetic route implied here for the synthesis of ZnS and CuS nanoparticles comprised of two phases; former as single source precursor and latter as liquid liquid interface method, which is quite cost effective as these can be carried out under ambient conditions. The synthesized particles were then characterized through UV-Vis analysis, Fourier transform infrared radiation (FTIR) and X-ray diffraction (XRD). The nanoparticles of ZnS prepared through liquid liquid interface were of 0.5-0.9nm and those of CuS were of 0.4-0.6 nm. The samples produced were used for the dye degradation of methylene blue with ZnS and CuS nanoparticles showing 89% and 91% degradation of organic dye respectively, both at the highest peak of 663 nm of UV-Vis analysis. Hence, on the bases of characteristics of these synthesized nanoparticles, it is suggested that these metal sulphide nanoparticles can be utilized for the removal of organic waste as dyes largely produced from textile industries and as novel semiconductors for solar applications.

Keywords: *nanoparticles, photo catalytic degradation, copper sulfide, zinc sulfide, semi-conductor*

Introduction

Nanotechnology has grabbed researchers in the topical era with the realistic approach that the nanometer sized substances even in one or more dimensions vividly modify their properties varied from those of bulk substances. There are separate mechanics to deal with both of them, as atoms and molecules through quantum mechanics while whole materials by classic mechanics. Nanometer range plays a threshold role in the distinct behavior of these domains. Metal NPs are significant subject of research because of their remarkably divergent properties and optical, thermal, catalytic, magnetic and sensor applications. The reduction of metal ions into solution is the frequently used method to synthesize metal NPs while the size and shape controlled synthesis mechanism is quite tricky and unclear yet (Chattopadhyay & Patel, 2012). The controlled synthesis of metal nanocrystals for various applications has been extensively studied in the last two decades. Recently, great efforts have been devoted to the controlled synthesis of thin nanostructures of metals, especially metal nanoplates and nanosheets (Fan et al., 2015). The semiconducting metal sulphides are extensively used for the synthesis and characterization of their nanocrystals being significantly potential in their properties and applications in the field of research. Due to the promising applications of these materials in electronics, data storage, energy storage, catalysis and sensors it is vital to cultivate simple, cost-effective, environment friendly, easily scalable and size and shape controlled synthetic routes (Sangma & Kalita, 2012).

Copper sulfide (Cu2S) is an important p-type semiconductor with great potential applications as cathode materials for lithium ion batteries, solar radiation absorbers and nonlinear optical materials (Lai et al., 2010). Cu2S has an extremely thin absorber layer in solar cells due to its nearly ideal bandgap of 1.2 eV and low cost. Cu2S is a mixed Cu ionic/electronic conductor and can also be used as nanoscale switches (Sakamoto et al., 2003 and Liu & Xue, 2011). Copper sulfides are the chalcogenide compounds belonging to the I-IV compound semiconductor materials having various applications in Nanosciences. Copper chalocogenides have fundamental applications in solar devices as valuable coatings in solar energy conversion systems and solar control devices. These are also used in the fabrication of microelectronic devices, remarkable optoelectronic properties e.g. as optical filters and in low temperature gas sensors. While recently the ternary copper chalcogenides like copper indium diselenide, and copper indium gallium selenides have found extensive use in the fabrication of solar photovoltaic cells (Offiah et al., 2012). Copper sulphide (CuS) has a variable stoichiometric composition as a semiconductor material. According to the literature the synthesized CuS nanocrystals exhibit strong emission peak at ~310 nm broad shoulder peaks at 404 nm and 466 nm (Priyadharshini & Revathy, 2015). The fascinating energy and catalytic applications of CuS NPs have engrossed the biomedical researchers around the world which is being quite vague front yet. While a steady and auspicious growth of CuS NPs is seen in photothermal therapy, drug delivery, sensing, molecular imaging and as multifunctional agents incorporating imaging and therapy (Qian et al., 2013). The physical and chemical characterization of the fabricated nanomaterials is essential as in case of CuS NPs it can deliver imperative knowledge of the elemental, structural and optical properties. There could be a wide range of characterization techniques with the major ones including X-Ray diffraction (XRD), scanning electron microscopy (SEM), energy dispersive X-Ray spectroscopy (EDS), transmission electron microscopy (TEM) and high resolution TEM (HRTEM), atomic force microscopy (AFM), Fourier transform infrared spectroscopy (FTIR), dynamic light scattering

(DLS), UV-visible and photoluminescence (PL) spectroscopy, etc. CuS NPs are extensively utilized in the detection of biomolecules e.g. DNA, metabolites such as glucose implied in diabetes and other diseases, food borne pathogens for prevention of food poisoning, hydrogen peroxide involved in many biomedical processes and pathways etc. The metallic electrical conduction and electron transfer reactions enhances the use of CuS NPs in sensing of biomolecules (Goel et al., 2014).

The degradation of chemicals and dyes through light radiation is arising as an interesting and attractive domain of energy and environmental subjects. Photocatalysts as semiconductor nanoparticles derive to be efficient components in this respect. Hence the nanomaterials with suitable band gap, chemical stability, non-toxicity and high photocatalytic activity are utilized for the photocatalytic degradation of excessively consumed harmful chemicals as dyes. Several metal sulfides have been conducted as catalysts for photodegradation purpose e.g. CdS, CuS, ZnS, MnS, Sb2S3, In2S3 etc. Currently several transition-metal sulfides as CuS and ZnS are studied extensively due to their unique optical properties. Copper Sulfide as photocatalysts is used directly for photocatalytic degradation (Thuy et al. 2014). Environmental surroundings are largely burdened of damaging chemicals, waste, gases and smoke due to swift mechanization. There are certain successful old methodologies to remove all type of wastes while Supercritical water oxidation (SCWO) proves to be a novel way to remove large organic waste far cheap than incineration or active carbon treatment. All the novel characteristics make them appropriate to degrade the unwanted from water and air. Afterwards these adsorbed particles can be removed through centrifugation or magnetic force (Khin et al., 2012). Methylene blue is an organic dye with a dark green odorless powder appearance at room temperature and a yield of blue solution in water. It's a heterocyclic aromatic chemical compound having a molecular formula as $C_{16}H_{18}ClN_3S$ (Tayade et al., 2009). Photocatalytic degradation of industrial wastewater through semiconductor nanoparticles is a green energy technique for the development and sustainability of environment (Sharma et al., 2016).

Experimental

First the required amount of amine as pyrrolidine $(CH_2)_4NH$ was taken to calculate its number of moles for further calculations. Available base Potassium Hydroxide (KOH) was weighed as by calculating the mass multiplying the molar mass of the base with that of the no. of moles of Pyrrolidine $(CH_2)_4NH$ and then added in Methanol (CH_3OH) solvent of approximate ratio as in the range of 60-100 ml by magnetic stirring in a three necked flask. After dissolving the base approximate 5ml amine Pyrrolidine $(CH_2)_4NH$ was added in the base solution while slightly magnetic stirring. Then Carbon Disulphide (CS_2) (also calculated by multiplying its molar mass with no. of moles of amine) was added in the solution while vigorously magnetic stirring. The solution changed its color from white to off white or yellowish white. The mass of metal nitrate as (Copper nitrate, zinc nitrate) taken was half of that taken of amine as Pyrrolidine $(CH_2)_4NH$ then dissolved in methanol solvent to prepare its homogenized mixture. It could also be filtered to improve the solubility of the metal nitrate solution. The metal nitrate solution was dropped while stirring in ligand. Metal complex obtained via above method was then filtered, recrystallized and left for drying. Liquid – liquid interface method was performed for the synthesis of nanoparticles. For this Toluene and distilled water were taken in same ratio 1:1. For this mass of metal complex was weighed and approximately taken and was divided by the molar mass of constituent ligand. The answer was then multiplied by specific ratio

defined for metal complex and sodium sulphide eg; 1:5 , 1:25, 1:30, 1:50 etc. Further answer was then multiplied with molar mass of sodium sulphide to obtain the mass in grams of sodium suphide for preparing its (Na_2S) solution in distilled water. Metal complex was added in the toluene to prepare a solution and then filtered to solubilize it completely. Distilled water and sodium sulphide solution was then freshly prepared, and was then added in metal complex and toluene solution with the help of dropper or syringe, dropwise along the wall of beaker carefully. Consequently an interface layer of nanoparticles was evolved in the solution. These reactions were repeatedly performed with reference to the variations of sodium sulfide concentration and time difference. Then with the help of dropper the above and below layer of liquid was separated and carefully shifted the interface layer in centrifuge tubes for centrifugation. The major layer containing particles was taken out in the same beakers and left for drying. The dried matter containing little impurity and particles were stored in ependrophs for further characterization and application. Photo degradation experiment was carried out using 0.01 g of Methylene blue dye solution in 1000 ml distilled water in a round bottom flask completely covered with foil paper. After stirring and preparation of uniform solution 100 ml aliquot was pipette out in two separate conical flasks. In one of the aliquot metal sulfide nanoparticle (CuS) was added while other was stored as reference. Then both of the samples were further directed for experimentation. First the UV-Vis analysis of the two aliquots was done and then they were kept in direct sunlight for 2hrs from 9 am to 11 am. After two hours the aliquots were again analyzed through UV-Vis and kept under sunlight for 4 hrs from 1 pm to 11:30 am to 3:30 pm. The practice was repeated for UV-Vis analysis and the aliquots were finally kept under sunlight for 6 hrs from 10 am to 4 pm on next day. The UV-Vis analysis was done for both samples. Decolorization was observed in the aliquots of dye containing nanoparticles samples. All the UV-Vis spectrums were then generated into graphs for further discussion of degradation results.

Results and Discussion

There were some techniques which were applied to characterize and analyse the synthesized nanoparticle material for further application as UV-Vis Analysis, Fourier transform infrared spectroscopy (**FTIR**) and X-ray powder diffraction (**XRD).** The results were further studied for the final discussion and analysis.

UV-VIS ANALYSIS

The UV-Vis photoelectric absorbance reading was obtained against required wavelength through UV machine (Model: UV- 1602, Company: Biotechnology Medical Science (BMS)) with a full scan of wavelength range 200-800 nm. After the analysis the graphs between wavelength and absorbance were added as they were while the excel data was incorporated to generate graphs on Origin 8 software by having E(eV) on X axis and direct band gap $(ahv)^2$ and indirect band gap $(ahv)^{1/2}$ on Y axis. A study reported the synthesis of CuS nanoparticles through sol gel route and their characterization done by UV-VIS absorption spectrum showed a hump at 429 nm depicting that the material atoms get excited to upper levels due to the absorption of UV radiation (Riyaz et al., 2016). The CuS NPs synthesized through two phase chemical route involving single source precursor and liquid liquid interface respectively in

different variations also represented first hump around 430 nm while shifting to higher absorption towards 300-200 nm in the blue shift referring to the nano regime. The variations arise preferably for the conditions, methodology and timing provided during synthesis procedure.

The first six samples (1-6) of CuS NPs were prepared with reference to the variation between CuS metal complex and Sodium Sulfide (Na_2S) ratio as 1:1, 1:20, 1:30, 1:40, 1:50 and 1:60 at constant time of 45 mins for the interface layer to generate following the liquid liquid interface method.

The next four samples (7-10) of CuS NPs were prepared with reference to the variation of time provided as 1 min, 5 mins, 15 mins and 30 mins with a constant ratio of CuS metal complex and sodium sulfide (Na_2S) of 1:40 for the interface layer to generate following the liquid liquid interface method. The present study also included the calculation of direct and indirect energy band gap of all the samples (1-10) of concentration and time variation as described above and further interpreted with previous research. According to statistical calculations the particles with hump at 429 nm have a direct band gap at 2.89 eV corresponding to the particles synthesized with different variations also representing the same measurements with even more greater band gap towards 3-4 eV reason being their greater blueshift towards 300-200 nm shown in Figure 1 (Riyaz et al., 2016).

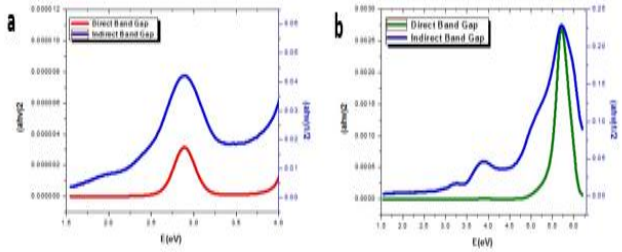

Figure 11 (a) Band Gap Graph of CuS 5 NP Sample synthesized with CuS Metal Complex and Sodium Sulfide (Na2S) variation in ratio of 1: 50 at constant time of 45 mins (b) Band Gap Graph of ZnS 7 NP Sample synthesized with ZnS Metal Complex and Sodium Sulfide (Na2S) constant in ratio of 1: 40 at time variation of 1 min

FOURIER TRANSFORM INFRARED (FTIR)

All infrared spectra were recorded in Shimadzu FT-IR 4000 Spectrophotometer using KBr pellet. A small portion of the sample was ground, mixed with ground KBr and pressed into a pellet in a hydraulic press applying a pressure of 40 pascal. The IR data was recorded as wavenumbers (cm^1) ranging from 400-4000. According to a research, CuS nanostructure had maximum peaks at 618 and the samples synthesized here also had peaks at the regime of 600-620 in agreement with the reported study (Riyaz et al., 2016). The prepared samples (1-10) of concentration and time variation having their peaks at respective wavenumbers in (cm^{-1}) are shown below in Figure 2.

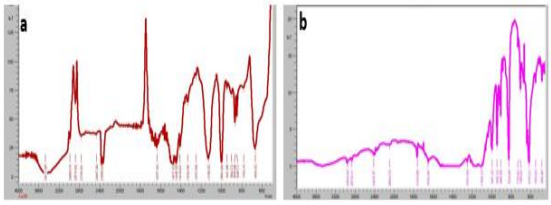

Figure 12 (a) CuS 5 NP Sample synthesized with CuS Metal Complex and Sodium Sulfide (Na2S) variation in ratio of 1: 50 at constant time of 45 mins (b) ZnS 7 NP Sample synthesized with ZnS Metal Complex and Sodium Sulfide (Na2S) constant in ratio of 1: 40 at time variation of 1 min

X-RAY DIFFRACTION ANALYSIS

The structural analysis was performed by using an X-ray diffractometer BRUKER D8. The X-ray generator was operated at 40 kV and 30 mA. The scanning regions of the diffraction angle (2θ) were 10^O to 60^O and Cu Kα radiation were used to collect the spectrum. The step interval was kept at 0.02^O with a scan rate of 75 secs. Average particle can be calculated from the XRD pattern using the well-known Debye-Scherrer formula given in the equation (Khan et al., 2013).

$$D = \frac{K\lambda}{\beta \cos\theta}$$

Where K is the Scherrer constant, λ is the wavelength of light used for the diffraction, β is the "full width at half maximum" of the sharp peaks, and θ is the angle measured. The Scherrer constant (K) in the above formula accounts for the shape of the particle and is generally taken to have the value 0.9 (Vinila et al., 2014). A study reported the XRD analysis of CuS nanostructures through X-ray diffractometer which can be indexed to hexagonal CuS structure as compared to the JCPDS database no. 78-0876. These particles had the size of 17.73 nm (Riyaz et al., 2016).

There are various routes to synthesize CuS NPs with different compositions and sizes. The CuS particles of less than 10nm in size lie in the blue shift of absorption spectrum and they have a strong quantum confinement effect. In a study single source precursor thermolysis produced larger CuS nanoparticles with a diameter of 21.7 nm and 26.0 nm. While another study revealed CuS nanocrystals declining from 5.9 nm to 2.9 nm in size refer to a certain blue shift in the UV-Vis absorption spectra from 1.3 eV to 1.6 eV (Roy and Srivastava, 2015).

The CuS NPs samples prepared through two phase route were also analysed through XRD and are indexed through JCPDS database no. 00-042-0564 and JCPDS database no. 01-072-0090 shown in Figure 3. While the particle size calculated through Debye-Scherrer formula ranged between 0.4-0.6 nm evidently in nanoregime as purposed in the literature reference.

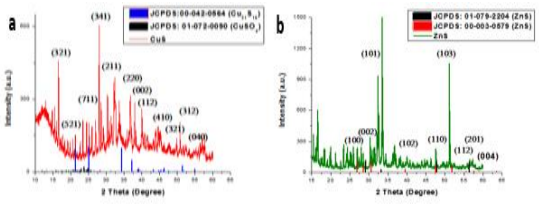

Figure 13 (a) XRD Analysis of CuS NP (b) XRD Analysis of ZnS NPs

Visible Light Directed Dye Degradation Analysis

According to a study reported methylene blue when dissolved in water showed three maxima peaks at 246, 291 and 663 nm for the UV-Vis spectrum. The absorption maxima wavelength of MB (λ_{max}) 291 and 663 nm) was used for the analysis during degradation and decolorization of MB dye, respectively (Tayade et al., 2009). The evaluation of photocatalytic activity of the prepared samples for the photocatalytic degradation of methylene blue dye performed under visible sun light. The wavelength absorbance maximum (λmax) of methylene is 663 nm as

above reported literature. Therefore, UV-Vis analysis for absorption of samples before and after exposure to visible light can be used for measurement of the % D (degradation efficiency of dye).

The decrease of absorbance value of samples at λmax of the dye after exposure in a certain time interval was shown at the rate of decolorization and therefore, photodegradation efficiency of the dye as well as the activity of nanoparticles as a photocatalyst. The decolorization and degradation efficiency (D) have been calculated as:

$$D = 100 \times \frac{A_o - A_t}{A_o}$$

Where, Ao is the initial absorbance of dye solution and At is the absorbance of the dye after exposure to visible sunlight in selected time interval.

The photodegradation of methylene blue dye was carried out in CuS and ZnS NPs separately under visible sunlight. Consequently, they exhibited prominent photocatalytic behavior for the degradation of methylene blue dye under solar visible sunlight exposure (Ayodhya & Veerabhadram, 2016). The graph generated in fig 8 shows the decline in absorption values with reference to three selected peak wavelengths in comparison of dye and dye with CuS NP sample simultaneously having a certain decline in values as the process of degradation proceeds.

The graph shown in fig 4 is between the highest peak with minimum absorption value and the sample of dye before exposure to visible light draws a clear graph showing the maximum absorption with reference to different time intervals.

The percentage degradation calculated for methylene blue dye done by CuS NPs was 91 % at the highest peak of 663 nm after exposure to visible light. Hence CuS NP resulted as an efficient and cost effective photocatalyst.

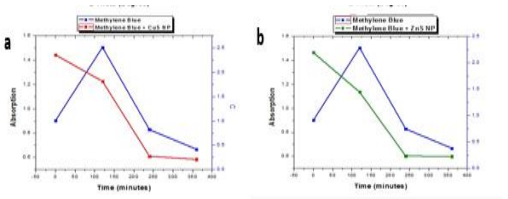

Figure 14 a) Comparison of Dye and Dye with ZnS NP Sample absorption value representing degradation at highest peak (663 nm) after exposure to 6hrs of visible sunlight (b) Comparison of Dye and Dye with CuS NP Sample absorption value representing degradation at highest peak (663 nm) after exposure to 6hrs of visible sunlight.

Conclusions

The nanoparticles of copper sulfide prepared through liquid liquid interface were of 0.4-0.6 nm. The synthetic route was quite cost effective and performed under normal conditions (e.g. temperature). The samples produced were used for the dye degradation of methylene blue with degradation results as CuS NPs showed 91% degradation. This method can be implied in future to utilize the metal sulfide nanoparticles for other novel applications maintain the ecological requirements and introducing new advancements. CuS NPs which were synthesized by a cost effective and efficient method were used to degrade dye of methylene blue. However on the bases of characteristics of these synthesized NPs, the present can

further recommends to be utilized for removing the organic waste as dyes largely produced from textile industries specifically.

ACKNOWLEDGMENT

We thank the U.S.-Pakistan Center for Advanced Studies in Energy, NUST Islamabad for their assistance in helping us carry out different test and analyses during our work. Thanks to the staff at Advanced Energy Materials & Systems laboratory at USPCAS-E, NUST for use of Powder X-ray diffraction system (PXRD), Thermogravimetric Analyzer (TGA) and Scanning Electron Microscopy (SEM).

References

1. Dhere, Neelkanth G. "Toward GW/Year Of CIGS Production Within The Next Decade". *Solar Energy Materials and Solar Cells* 91.15-16 (2007): 1376-1382. Web.
2. Chapin, D. M., Fuller, C. S. and Pearson, G. L. "A New Silicon p-n Junction Photocell for Converting Solar Radiation into Electrical Power," *Journal of Applied Physics* Vol. 25 (May 1954) pp. 676-77.
3. Bar, H., Bhui, D., Sahoo, G., Sarkar, P., De, S., & Misra, A. (2009). Green synthesis of silver nanoparticles using latex of Jatropha curcas. *Colloids And Surfaces A: Physicochemical And Engineering Aspects*, *339*(1-3), 134-139. http://dx.doi.org/10.1016/j.colsurfa.2009.02.008
4. Zou, C., Zhang, L., Lin, D., Yang, Y., Li, Q., Xu, X., ... & Huang, S. (2011). Facile synthesis of Cu 2 ZnSnS 4 nanocrystals. *CrystEngComm*, *13*(10), 3310-3313.
5. Chen, G., Zhu, F., Sun, X., Sun, S., & Chen, R. (2011). Benign synthesis of ceria hollow nanocrystals by a template-free method. *CrystEngComm*, *13*(8), 2904-2908.
6. Tarascon, J. M., & Armand, M. (2001). Issues and challenges facing rechargeable lithium batteries. *Nature*, *414*(6861), 359-367.
7. Whittingham, M. S. (2004). Lithium batteries and cathode materials. *Chemical reviews*, *104*(10), 4271-4302.
8. Arico, A. S., Bruce, P., Scrosati, B., Tarascon, J. M., & Van Schalkwijk, W. (2005). Nanostructured materials for advanced energy conversion and storage devices. *Nature materials*, *4*(5), 366-377.
9. Simon, P., & Gogotsi, Y. (2008). Materials for electrochemical capacitors. *Nature materials*, *7*(11), 845-854.
10. Liu, C., Li, F., Ma, L. P., & Cheng, H. M. (2010). Advanced materials for energy storage. *Advanced materials*, *22*(8).
11. Niu, Z., Zhang, L., Liu, L., Zhu, B., Dong, H., & Chen, X. (2013). All- Solid- State Flexible Ultrathin Micro- Supercapacitors Based on Graphene. *Advanced Materials*, *25*(29), 4035-4042.
12. Niu, Z., Luan, P., Shao, Q., Dong, H., Li, J., Chen, J., ... & Xie, S. (2012). A “skeleton/skin” strategy for preparing ultrathin free-standing single-walled carbon nanotube/polyaniline films for high performance supercapacitor electrodes. *Energy & Environmental Science*, *5*(9), 8726-8733.
13. Dong, X., Ma, Y., Zhu, G., Huang, Y., Wang, J., Chan-Park, M. B., ... & Chen, P. (2012). Synthesis of graphene–carbon nanotube hybrid foam and its use as a novel

three-dimensional electrode for electrochemical sensing. *Journal of Materials Chemistry*, *22*(33), 17044-17048.

14. Lai, C. H., Lu, M. Y., & Chen, L. J. (2012). Metal sulfide nanostructures: synthesis, properties and applications in energy conversion and storage. *Journal of Materials Chemistry*, *22*(1), 19-30.
15. Shen, S., & Wang, Q. (2012). Rational tuning the optical properties of metal sulfide nanocrystals and their applications. *Chemistry of Materials*, *25*(8), 1166-1178.
16. Harrison, M. R., & Francesconi, M. G. (2011). Mixed-metal one-dimensional sulfides—A class of materials with differences and similarities to oxides. *Coordination Chemistry Reviews*, *255*(3), 451-458.
17. Zhang, F., & Wong, S. S. (2009). Controlled synthesis of semiconducting metal sulfide nanowires. *Chemistry of materials*, *21*(19), 4541-4554.
18. Seo, J. W., Jun, Y. W., Park, S. W., Nah, H., Moon, T., Park, B., ... & Cheon, J. (2007). Two- Dimensional Nanosheet Crystals. *Angewandte Chemie International Edition*, *46*(46), 8828-8831.
19. Goriparti, S., Miele, E., De Angelis, F., Di Fabrizio, E., Zaccaria, R. P., & Capiglia, C. (2014). Review on recent progress of nanostructured anode materials for Li-ion batteries. *Journal of Power Sources*, *257*, 421-443.
20. Kim, Y., & Goodenough, J. B. (2008). Lithium insertion into transition-metal monosulfides: tuning the position of the metal 4s band. *The Journal of Physical Chemistry C*, *112*(38), 15060-15064.
21. Bruce, P. G., Scrosati, B., & Tarascon, J. M. (2008). Nanomaterials for rechargeable lithium batteries. *Angewandte Chemie International Edition*, *47*(16), 2930-2946.
22. Kaviya, S., Santhanalakshmi, J., & Viswanathan, B. (2011). Green Synthesis of Silver Nanoparticles Using Polyalthia longifolia Leaf Extract along with D-Sorbitol: Study of Antibacterial Activity. *Journal Of Nanotechnology*, 1-5. http://dx.doi.org/10.1155/2011/152970
23. Wang, X., Zhuang, J., Peng, Q., & Li, Y. (2005). A general strategy for nanocrystal synthesis. *Nature*, *437*(7055), 121-124. http://dx.doi.org/10.1038/nature03968
24. Chattopadhyay, D. P., & Patel, B. H. (2012). Preparation, characterization and stabilization of nano sized copper particles. *International Journal of Pure Sciences and Technology*, *9*(1), 1-8.
25. Chen, K. C., Wu, W. W., Liao, C. N., Chen, L. J., & Tu, K. N. (2008). Observation of atomic diffusion at twin-modified grain boundaries in copper. *Science*, *321*(5892), 1066-1069.
26. Law, M., Greene, L. E., Johnson, J. C., Saykally, R., & Yang, P. (2005). Nanowire dye-sensitized solar cells. *Nature materials*, *4*(6), 455-459.
27. Dandia, Anshu et al. "ZnS Nanoparticle Catalysed Four Component Syntheses Of Novel Spiropolyhydroquinoline Derivatives In Aqueous Medium Under Ultrasonic Irradiation". *Proc. Natl. Acad. Sci., India, Sect. A Phys. Sci.* 85.1 (2014): 19-27. Web.
28. Dyal, C., Nguyen, N., Hadden, J., Gou, L., Tan, L., Murphy, C. J., ... & Nivens, D. (2006, March). Green Synthesis of Gold and Silver Nanoparticles from Plant Extracts. In *ABSTRACTS OF PAPERS OF THE AMERICAN CHEMICAL SOCIETY* (Vol. 231). 1155 16TH ST, NW, WASHINGTON, DC 20036 USA: AMER CHEMICAL SOC.

U. Jamil, 2018/ (Aug 15-16, 2018); COMSATS Institute of Information Technology, Islamabad, Pakistan

29. Fan, Z., Huang, X., Tan, C., & Zhang, H. (2015). Thin metal nanostructures: synthesis, properties and applications. *Chem. Sci.*, *6*(1), 95-111. http://dx.doi.org/10.1039/c4sc02571g
30. Xu, Z., Zeng, Q., Lu, G., & Yu, A. (2006). Inorganic nanoparticles as carriers for efficient cellular delivery. *Chemical Engineering Science*, *61*(3), 1027-1040. http://dx.doi.org/10.1016/j.ces.
31. Sultan, Muhammad et al. (2012) "Hexanuclear Copper–Nickel And Copper–Cobalt Complexes For Thin Film Deposition Of Ceramic Oxide Composites". New J. Chem. 36.4:911. Web.
32. Ramasamy, K., Malik, M. A., Revaprasadu, N., & O'Brien, P. (2013). Routes to nanostructured inorganic materials with potential for solar energy applications. *Chemistry of Materials*, *25*(18), 3551-3569.
33. Alivisatos, A. P. (1996). Semiconductor clusters, nanocrystals, and quantum dots. *Science*, *271*(5251), 933.
34. Ma, D. D. D., Lee, C. S., Au, F. C. K., Tong, S. Y., & Lee, S. T. (2003). Small-diameter silicon nanowire surfaces. *Science*, *299*(5614), 1874-1877.
35. Wang, Z. L., & Song, J. (2006). Piezoelectric nanogenerators based on zinc oxide nanowire arrays. *Science*, *312*(5771), 242-246.
36. Fang, X., Bando, Y., Gautam, U. K., Zhai, T., Gradečak, S., & Golberg, D. (2009). Heterostructures and superlattices in one-dimensional nanoscale semiconductors. *Journal of Materials Chemistry*, *19*(32), 5683-5689.
37. Lai, C. H., Huang, K. W., Cheng, J. H., Lee, C. Y., Hwang, B. J., & Chen, L. J. (2010). Direct growth of high-rate capability and high capacity copper sulfide nanowire array cathodes for lithium-ion batteries. *Journal of Materials Chemistry*, *20*(32), 6638-6645.
38. Chen, L. J. (2007). Silicon nanowires: the key building block for future electronic devices. *Journal of Materials Chemistry*, *17*(44), 4639-4643.
39. Chen, L. J. (2005). Metal silicides: An integral part of microelectronics. *Jom*, *57*(9), 24-30.
40. Zhu, Junjie et al. 2001) "Preparation Of Cds And Zns Nanoparticles Using Microwave Irradiation". *Materials Letters* 47.1-2 (2001): 25-29. Web.
41. Sangma, A. D., & Kalita, P. K. (2012). Chemical synthesis of metal doped copper sulphide nanoparticles in PVA matrix.
42. Huang, K. W., Wang, J. H., Chen, H. C., Hsu, H. C., Chang, Y. C., Lu, M. Y., ... & Chen, L. J. (2007). Supramolecular nanotubes with high thermal stability: a rigidity enhanced structure transformation induced by electron-beam irradiation and heat. *Journal of Materials Chemistry*, *17*(22), 2307-2312.
43. Wen, Z., & Li, J. (2009). Hierarchically structured carbon nanocomposites as electrode materials for electrochemical energy storage, conversion and biosensor systems. *Journal of Materials Chemistry*, *19*(46), 8707-8713.
44. Wu, Y., Wadia, C., Ma, W., Sadtler, B., & Alivisatos, A. P. (2008). Synthesis and photovoltaic application of copper (I) sulfide nanocrystals. *Nano letters*, *8*(8), 2551-2555.
45. Li, T. L., Lee, Y. L., & Teng, H. (2011). CuInS2 quantum dots coated with CdS as high-performance sensitizers for TiO2 electrodes in photoelectrochemical cells. *Journal of Materials Chemistry*, *21*(13), 5089-5098.

U. Jamil, 2018/ (Aug 15-16, 2018); COMSATS Institute of Information Technology, Islamabad, Pakistan

46. Bierman, M. J., & Jin, S. (2009). Potential applications of hierarchical branching nanowires in solar energy conversion. *Energy & Environmental Science*, *2*(10), 1050-1059.
47. Moore, D., & Wang, Z. L. (2006). Growth of anisotropic one-dimensional ZnS nanostructures. *Journal of Materials Chemistry*, *16*(40), 3898-3905.
48. Fang, X. S., Bando, Y., Shen, G. Z., Ye, C. H., Gautam, U. K., Costa, P. M., ... & Golberg, D. (2007). Ultrafine ZnS nanobelts as field emitters. *Advanced Materials*, *19*(18), 2593-2596.
49. Lu, M. Y., Lu, M. P., Chung, Y. A., Chen, M. J., Wang, Z. L., & Chen, L. J. (2009). Intercrossed sheet-like Ga-doped ZnS nanostructures with superb photocatalytic actvitiy and photoresponse. *The Journal of Physical Chemistry C*, *113*(29), 12878-12882.
50. Lai, C. H., Huang, K. W., Cheng, J. H., Lee, C. Y., Hwang, B. J., & Chen, L. J. (2010). Direct growth of high-rate capability and high capacity copper sulfide nanowire array cathodes for lithium-ion batteries. *Journal of Materials Chemistry*, *20*(32), 6638-6645.
51. Sakamoto, T., Sunamura, H., Kawaura, H., Hasegawa, T., Nakayama, T., & Aono, M. (2003). Nanometer-scale switches using copper sulfide. *Applied physics letters*, *82*(18), 3032-3034.
52. Liu, J., & Xue, D. (2011). Rapid and scalable route to CuS biosensors: a microwave-assisted Cu-complex transformation into CuS nanotubes for ultrasensitive nonenzymatic glucose sensor. *Journal of Materials Chemistry*, *21*(1), 223-228.
53. Jiang, Y., Zhang, W. J., Jie, J. S., Meng, X. M., Zapien, J. A., & Lee, S. T. (2006). Homoepitaxial growth and lasing properties of ZnS nanowire and nanoribbon arrays. *Advanced Materials*, *18*(12), 1527-1532.
54. Moore, D., & Wang, Z. L. (2006). Growth of anisotropic one-dimensional ZnS nanostructures. *Journal of Materials Chemistry*, *16*(40), 3898-3905.
55. Lai, Chen-Ho, Ming-Yen Lu, and Lih-Juann Chen. "Metal Sulfide Nanostructures: Synthesis, Properties And Applications In Energy Conversion And Storage". *J. Mater. Chem*. 22.1 (2012): 19-30. Web.
56. Khan, Malik Dilshad et al. "Phase-Pure Fabrication And Shape Evolution Studies Of Sns Nanosheets". *New J. Chem*. 39.12 (2015): 9569-9574. Web.
57. Fleet, M. E. (2006). Phase equilibria at high temperatures. *Reviews in mineralogy and geochemistry*, *61*(1), 365-419.
58. Offiah, S. U., Ugwoke, P. E., Ekwealor, A. B. C., Ezugwu, S. C., Osuji, R. U., & Ezema, F. I. (2012). Structural and spectral analysis of chemical bath deposited copper sulfide thin films for solar energy conversions. *Digest Journal Of Nano Materials And Bio Structures*, *7*(1), 165-173.
59. Priyadharshini P and Revathy Rajagopal., Synthesis and Characterization of Metal doped Nanocrystallinecopper Sulphide. *International Journal of Recent Scientific Research Vol. 6, Issue, 4, pp.3328-3331, April, 2015*
60. Lu, Q., Gao, F., & Zhao, D. (2002). One-step synthesis and assembly of copper sulfide nanoparticles to nanowires, nanotubes, and nanovesicles by a simple organic amine-assisted hydrothermal process. *Nano Letters*, *2*(7), 725-728.
61. Feigl, Christopher A., Amanda S. Barnard, and Salvy P. Russo. (2012) "Size- And Shape-Dependent Phase Transformations In Wurtzite Zns Nanostructures". *Phys. Chem. Chem. Phys.* 14.28: 9871. Web.

U. Jamil, 2018/ (Aug 15-16, 2018); COMSATS Institute of Information Technology, Islamabad, Pakistan

62. Rathore, K. S., Patidar, D., Janu, Y., Saxena, N. S., Sharma, K., & Sharma, T. P. (2008). Structural and optical characterization of chemically synthesized ZnS nanoparticles. *Chalcogenide Letters*, *5*(6), 105-110.
63. Borah, J. P., Barman, J., & Sarma, K. C. (2008). Structural and optical properties of ZnS nanoparticles. *Chalcogenide Lett*, *5*(9), 201-208.
64. Maheshwari, V. C. (2006). Large area electro-optical tactile sensor: Characterization and design of a polymer, nanoparticle based tunneling device.
65. Abbas, N. K., Al-Rasoul, K. T., & Shanan, Z. J. (2013). New method of preparation ZnS Nano size at low pH. *Int. J. Electrochem. Sci*, *8*, 3049-3056.
66. Rui, X., Tan, H., & Yan, Q. (2014). Nanostructured metal sulfides for energy storage. *Nanoscale*, *6*(17), 9889-9924.
67. Xiao, G., Wang, Y., Ning, J., Wei, Y., Liu, B., & Yu, W. et al. (2013). Recent advances in IV–VI semiconductor nanocrystals: synthesis, mechanism, and applications. *RSC Advances*, *3*(22), 8104. http://dx.doi.org/10.1039/c3ra23209c
68. Doria, G., Conde, J., Veigas, B., Giestas, L., Almeida, C., Assunção, M., ... & Baptista, P. V. (2012). Noble metal nanoparticles for biosensing applications. *Sensors*, *12*(2), 1657-1687.
69. Zhang, Y., Hong, H., Myklejord, D. V., & Cai, W. (2011). Molecular Imaging with SERS- Active Nanoparticles. *Small*, *7*(23), 3261-3269.
70. Cai, W., & Hong, H. (2012). Invited Perspective In a "nutshell": intrinsically radio-labeled quantum dots. *Am J Nucl Med Mol Imaging*, *2*(2), 136-140.
71. Yigit, M. V., & Medarova, Z. (2012). In vivo and ex vivo applications of gold nanoparticles for biomedical SERS imaging. *Am J Nucl Med Mol Imaging*, *2*(2), 232-241.
72. Qian, L., Mao, J., Tian, X., Yuan, H., & Xiao, D. (2013). In situ synthesis of CuS nanotubes on Cu electrode for sensitive nonenzymatic glucose sensor. *Sensors and Actuators B: Chemical*, *176*, 952-959.
73. Ghosh Chaudhuri, R., & Paria, S. (2011). Core/shell nanoparticles: classes, properties, synthesis mechanisms, characterization, and applications. *Chemical reviews*, *112*(4), 2373-2433.
74. Goel, S., Chen, F., & Cai, W. (2014). Synthesis and biomedical applications of copper sulfide nanoparticles: from sensors to theranostics. *Small*, *10*(4), 631-645.
75. Borah, J. P., Barman, J., & Sarma, K. C. (2008). Structural and optical properties of ZnS nanoparticles. *Chalcogenide Lett*, *5*(9), 201-208.
76. Gottschalk, F., & Nowack, B. (2011). The release of engineered nanomaterials to the environment. *Journal of Environmental Monitoring*, *13*(5), 1145-1155.
77. Kaegi, R., Voegelin, A., Sinnet, B., Zuleeg, S., Hagendorfer, H., Burkhardt, M., & Siegrist, H. (2011). Behavior of metallic silver nanoparticles in a pilot wastewater treatment plant. *Environmental science & technology*, *45*(9), 3902-3908.
78. Christian, P., Von der Kammer, F., Baalousha, M., & Hofmann, T. (2008). Nanoparticles: structure, properties, preparation and behaviour in environmental media. *Ecotoxicology*, *17*(5), 326-343.
79. Shimose, H., Singh, M., Ahuja, D., Zhao, W., Shan, S., Nishino, S., ... & Luo, J. (2016). Copper Sulfide–Zinc Sulfide Janus Nanoparticles and Their Seebeck Characteristics for Sustainable Thermoelectric Materials. *The Journal of Physical Chemistry C*, *120*(11), 5869-5875.

U. Jamil, 2018/ (Aug 15-16, 2018); COMSATS Institute of Information Technology, Islamabad, Pakistan

80. Crini, G., Peindy, H. N., Gimbert, F., & Robert, C. (2007). Removal of CI Basic Green 4 (Malachite Green) from aqueous solutions by adsorption using cyclodextrin-based adsorbent: Kinetic and equilibrium studies. *Separation and Purification Technology*, *53*(1), 97-110.
81. Subash, B., Krishnakumar, B., Sobral, A. J., Surya, C., John, N. A. A., Senthilraja, A., ... & Shanthi, M. (2016). Synthesis, characterization and daylight active photocatalyst with antiphotocorrosive property for detoxification of azo dyes. *Separation and Purification Technology*, *164*, 170-181.
82. Fang, X., Zhai, T., Gautam, U. K., Li, L., Wu, L., Bando, Y., & Golberg, D. (2011). ZnS nanostructures: from synthesis to applications. *Progress in Materials Science*, *56*(2), 175-287.
83. Thuy, U. T. D., Liem, N. Q., Parlett, C. M., Lalev, G. M., & Wilson, K. (2014). Synthesis of CuS and CuS/ZnS core/shell nanocrystals for photocatalytic degradation of dyes under visible light. *Catalysis Communications*, *44*, 62-67.
84. Tayade, R. J., Natarajan, T. S., & Bajaj, H. C. (2009). Photocatalytic degradation of methylene blue dye using ultraviolet light emitting diodes. *Industrial & Engineering Chemistry Research*, *48*(23), 10262-10267.
85. Sharma, Surbhi, Simrjit Singh, and Neeraj Khare. "Synthesis Of Polyaniline/Cds (Nanoflowers And Nanorods) Nanocomposites: A Comparative Study Towards Enhanced Photocatalytic Activity For Degradation Of Organic Dye". *Colloid Polym Sci* 294.5 (2016): 917-926. Web.
86. Khin, M. M., Nair, A. S., Babu, V. J., Murugan, R., & Ramakrishna, S. (2012). A review on nanomaterials for environmental remediation. *Energy & Environmental Science*, *5*(8), 8075-8109.
87. Riyaz, S., Parveen, A., Azam, A.,Microstructural and Optical Properties of CuS Nanoparticles prepared by Sol Gel route, *Perspectives in Science* (2016), http://dx.doi.org/10.1016/j.pisc.2016.06.041
88. Borah, J. P., Barman, J., & Sarma, K. C. (2008). Structural and optical properties of ZnS nanoparticles. *Chalcogenide Lett*, *5*(9), 201-208.
89. Bahadur, J., Agrawal, S., Parveen, A., Jawad, A., Ashraf, S. S. Z., & Ghalib, R. M. (2015). Micro-Structural, Optical and Dielectric Properties of Ag Doped TiO2 Synthesized by Sol–Gel Method. *Materials Focus*, *4*(2), 134-141.
90. Riyaz, S., Parveen, A., Azam, A.,Microstructural and Optical Properties of CuS Nanoparticles prepared by Sol Gel route, *Perspectives in Science* (2016), http://dx.doi.org/10.1016/j.pisc.2016.06.041
91. Malarkodi, C., & Annadurai, G. (2013). A novel biological approach on extracellular synthesis and characterization of semiconductor zinc sulfide nanoparticles. *Applied Nanoscience*, *3*(5), 389-395.
92. Khan, E. M., Alam, F., Parveen, A., & Naqvi, A. H. (2013). Structural, optical and dielectric properties of alkaline earth metal (Sr0. 05, Mg0. 05 and Ba0. 05) doped CaF2 nanoparticles and their microscopic analysis. *Journal of Advanced Microscopy Research*, *8*(1), 45-52.
93. Vinila, V. S. et al. "XRD Studies On Nano Crystalline Ceramic Superconductor Pbsrcacuo At Different Treating Temperatures". *CSTA* 03.01 (2014): 1-9. Web.
94. Riyaz, S., Parveen, A., Azam, A.,Microstructural and Optical Properties of CuS Nanoparticles prepared by Sol Gel route, *Perspectives in Science* (2016), http://dx.doi.org/10.1016/j.pisc.2016.06.041

U. Jamil, 2018/ (Aug 15-16, 2018); COMSATS Institute of Information Technology, Islamabad, Pakistan

95. Roy, P., & Srivastava, S. K. (2015). Nanostructured anode materials for lithium ion batteries. *Journal of Materials Chemistry A*, *3*(6), 2454-2484.
96. Borah, J. P., Barman, J., & Sarma, K. C. (2008). Structural and optical properties of ZnS nanoparticles. *Chalcogenide Lett*, *5*(9), 201-208.
97. Tayade, R. J., Natarajan, T. S., & Bajaj, H. C. (2009). Photocatalytic degradation of methylene blue dye using ultraviolet light emitting diodes. *Industrial & Engineering Chemistry Research*, *48*(23), 10262-10267.